Exploiting PP2A dependent and independent effects of forskolin for therapeutic targeting of KMT2A (MLL)-rearranged acute leukaemia

Received: 19 July 2024 | Revised: 3 June 2025 | Accepted: 6 July 2025

DOI: 10.1111/bph.70158

RESEARCH ARTICLE

'Exploiting PP2A dependent and independent effects of forskolin for therapeutic targeting of KMT2A (MLL)-rearranged acute leukaemia'

Yoana Arroyo-Berdugo[1] | Antonella Di Mambro[1] | Volker Behrends[2] | Michelle A. Sahai[3] | Luca Cozzuto[4] | Immacolata Zollo[5] | Julia Ponomarenko[4,6] | Owen Williams[7] | John Gribben[8] | Yolanda Calle[1] | Bela Patel[8] | Maria Teresa Esposito[1,9]

[1]School of Life and Health Sciences, University of Roehampton, London, UK

[2]School of Biomedical Sciences, University of West London, London, UK

[3]Division of Biosciences, Department of Life Sciences, College of Health and Life Sciences, Brunel University of London, Uxbridge, UK

[4]Centre Genomic Regulation, CRG, Barcelona, Spain

[5]CEINGE Biotecnologie Avanzate, Naples, Italy

[6]University Pompeu Fabra (UPF), Barcelona, Spain

[7]Great Ormond Street Institute of Child Health London, UCL, London, UK

[8]Barts Cancer Institute, Queen Mary University of London, London, UK

[9]School of Biosciences, University of Surrey, Guildford, UK

Correspondence
Maria Teresa Esposito, School of Biosciences, University of Surrey, Guildford, UK.
Email: mariateresa.esposito@surrey.ac.uk

Funding information
This project has been supported by Leukaemia UK (John Goldman fellowship), the Institute of Biomedical Science, the University of Roehampton and the University of Surrey.

Background and Purpose: Activation of Protein Phosphatase 2A (PP2A), via genetic and pharmacologic modulation of SET, has recently being identified as a promising strategy to therapeutically target acute myeloid leukaemia (AML) carrying *KMT2A (MLL)* chromosomal translocations (*KMT2A*-r AML).

Experimental Approach: In this study, we investigated the expression of PP2A subunits and the therapeutic potential of forskolin, a cyclic adenosine monophosphate (cAMP) elevating natural compound that has been reported as a PP2A activator.

Key Results: Our data show that *PPP2CA* encoding protein phosphatase 2 catalytic subunit α is abundantly expressed in *KMT2A*-r AML cells. Treatment with forskolin arrests proliferation; induces cell death; represses the expression of *MYC*, *HOXA9* and *HOXA10*; stimulates PP2A activity; and attenuates the activity of ERK1/2 in *KMT2A*-r AML cells. Forskolin increases sensitivity to standard-of-care daunorubicin in *KMT2A*-AML cell lines and PDX. Silencing *PPP2CA* partially rescues the cytotoxic effect of forskolin, stimulates ERK1/2, inhibits GSK3β, and abolishes the forskolin-mediated repression of c-*MYC* and *HOXA10*, but it did not affect the potentiation of response to daunorubicin. This effect was also not dependent on increase of cAMP, but it was because of increase in the intracellular accumulation of daunorubicin, through inhibition of drug efflux pump P-glycoprotein 1 (multidrug resistance protein).

Conclusions and Implications: In conclusion, our findings highlight a novel mechanism of action for forskolin and support a potential role of this natural compound in combination with current conventional agent daunorubicin in the treatment of *KMT2A*-r AML.

Abbreviations: AML, acute myeloid leukaemia; Cryo-EM, Cryo electron miscroscopy; eGFP, enhanced green fluorescence protein; FBS, fetal bovine serum; GFP, green fluorescence protein; KMT2A, Histone-lysine *N*-methyltransferase 2A; MDR, multi-drug resistance protein; OA, okadaic acid; PDX, patient-derived xenotransplant; pGP, p-glycoprotein 1; pNPP, *para*-Nitrophenylphosphate; RPMI-1640 medium, Roswell park memorial institute-1640 medium; TBS, TRIS buffer saline.

KEYWORDS
AML, daunorubicin, ERK1/2, forskolin, GSK3β, HOXA, KMT2A, leukaemia, MDR, MLL, MYC, natural compounds, P-glycoprotein, phosphatase, PP2A

1 | INTRODUCTION

Acute myeloid leukaemia (AML) is a heterogeneous disease characterised by blocked differentiation and increased proliferation of haematopoietic progenitors sustained by leukaemia stem cells (LSC) that, like haematopoietic stem cells (HSC) in the development of blood cells, maintain and regenerate leukaemia owing to their ability of unlimited self-renewal. The heterogeneity of AML can be attributed to diverse driver genetic mutations that may be present in combination with epigenetic abnormalities (Tazi et al., 2022). Among these, 11q23 chromosomal translocations affecting the gene *KMT2A*, encoding for **Histone 3 lysine 4 methyltransferase**, represent a potent driver mutation, associated with resistance to chemotherapy and very poor prognosis (M. Esposito, 2019; Meyer et al., 2023; Winters & Bernt, 2017). Therapies targeting the genetic drivers have improved the outcomes of some AML patients' subsets; however, these therapeutic strategies are limited to patients with a clear actionable driver mutation or chromosomal rearrangement (Dohner et al., 2021). Proteomic and phospho-proteomic approaches have complemented the genomic studies, elucidating deregulated signalling networks and identifying protein kinases as key druggable drivers of AML (Aasebo et al., 2020; Casado et al., 2023; Gosline et al., 2022; Kramer et al., 2022). Accordingly, small molecules kinase inhibitors have been developed and tested in AML models (Takahashi, 2023). However, most of these inhibitors have a toxicity which is clinically prohibitive; others, when tested in clinical trials, only resulted in non-sustained responses, suggesting the existence of redundancy mechanisms (Takahashi, 2023). Novel therapies are being designed to target multiple kinase pathways at the same time. However, the toxicity of the most promising kinase inhibitors hampers the clinical feasibility and success of this multi-targeting approach. Therefore, alternative therapeutic approaches are needed. Whereas kinases have been at the heart of cancer drug discovery projects, protein phosphatases are less studied. Among these, **serine/threonine phosphatase PP2A** has emerged as a critical tumour suppressor regulating a vast portion of the phosphoproteome, whose inactivation contributes to the development of cancer (Kauko & Westermarck, 2018). Somatic mutations and deletions of the *PPP2CA* gene, encoding the catalytic subunit α isoform of PP2A, have been found in several solid tumours and in myelodysplastic syndrome; however, they have never been reported in leukaemia (Kandoth et al., 2013). Nevertheless, PP2A is functionally inactivated in over 70% of AML cases (Cristobal et al., 2011), as a result of over-expression of endogenous inhibitors as well as aberrant expression of structural and regulatory subunits (Ramaswamy et al., 2015). We and others have shown that the PP2A activator **FTY720** has therapeutic efficacy in pre-clinical models of AML, in particular in *KMT2A*-r AML; however, the immunosuppressive nature of FTY720 precludes its clinical translation (Di Mambro et al., 2023; Di Mambro & Esposito, 2022; Goswami et al., 2022). Here, we investigated the expression of PP2A subunits in AML and the therapeutic activity of a natural diterpene, the adenylate cyclase agonist **forskolin**, as a PP2A activator. Our results indicate that forskolin has a cytostatic effect, and it potentiates the response to standard-of-care **daunorubicin** in *KMT2A*-r AML. We elucidate forskolin's mechanisms of action as both dependent and independent of PP2A.

What is already known?

- PP2A has been identified as a therapeutic target for acute myeloid leukaemia (AML).
- Forskolin, a putative PP2A activator, has anti-cancer effects.

What does this study add?

- The study identifies a cytostatic and cytotoxic effect of forskolin on KMT2A-r leukaemic cells.
- Forskolin shows unanticipated, PP2A-independent, sensitising activity to daunorubicin.

What is the clinical significance?

- PP2A re-activation via forskolin is a therapeutic strategy for KMT2A-r AML.
- Forskolin could be employed to improve the therapeutic index and tolerability of daunorubicin.

2 | METHODS

The report of the material and methods described in this paper comply to the guidelines set out by Izzo et al. (2020). The experimental design and analysis of data comply with guidelines set out by Curtis et al. (2025).

2.1 | Cell lines

The cells lines used for this study and their culture conditions are described in Arroyo-Berdugo et al. (2023) and Di Mambro et al. (2023) and Table S1. The cell lines K562 (DSMZ AAC10, RRID: CVCL_0004), MV4-11 (DSMZ ACC102, RRID CVCL_0064) and THP1 (DSMZ ACC16, CVCL_0006) were grown in Roswell Park Memorial Institute medium (RPMI-1640) (Sigma-Merck, Haverill, UK) supplemented with 10% of fetal bovine serum (FBS) and 100 U ml^{-1} penicillin and 100 μg ml^{-1} streptomycin; Kasumi1 (DSMZ ACC220, RRID: CVCL_0589) were grown in RPMI-1640, 25 mM HEPES-modified and supplemented with 20% of FBS and 100 U ml^{-1} penicillin and 100 μg ml^{-1} streptomycin; and HS5 were grown in DMEM and supplemented with 10% of FBS and 100 U ml^{-1} penicillin and 100 μg ml^{-1} streptomycin. All the cell lines were maintained in culture at 37°C in a 5% CO_2, by routine passage every 2–3 days and regularly tested for mycoplasma contamination using PCR Mycoplasma detection kit from Applied Biological Materials (Abm). These cell lines were further tested for authenticity by STR profiling (Eurofin Genomics, London UK) in July 2023.

The leukaemic cell lines used for drug treatment were stably transduced with a lentivirus vector expressing the enhanced green fluorescent protein (eGFP). The stromal cell line HS5 (ATCC CRL-3611, RRID: CVCL_3720) was stably transduced with a lentivirus vector expressing the monomer cherry (mcherry) (Arroyo-Berdugo et al., 2023).

2.2 | Primary cells

Primary samples, described in Di Mambro et al. (2023) and Tables S2 and S3, were obtained from the Cancer Tissue Bank at the Barts Cancer Institute (London, UK) under ethical approval (REC reference: 17/WM/0428).

2.3 | Patient-derived xenotransplant (PDX) samples

The KMT2A-PDX, described in Di Mambro et al. (2023), were a generous gift of Professor Owen Williams. The sample identified as 1547 was an AML sample carrying t(9;11) and isolated in Rotterdam (NE). The sample 270418A was an AML sample carrying t(11;19) and isolated at GOSH (London, UK). These cells were grown in MethoCult H4435 (Stem Cell Technologies, Cambridge UK) with addition of 10 ng ml^{-1} human TPO1 and human FLt3 ligand (Stem Cell Technologies, Cambridge UK).

2.4 | Virus production and cell transduction

Knock-down of *PPP2CA* was conducted in vitro using the lentiviral viruses purchased from Sigma–Merck (Haverill, UK), as described in Di Mambro et al. (2023). The sequence of the hairpin is described in Table S4.

2.5 | Cell proliferation and cell death analysis

Cell proliferation and cell death were monitored by GFP fluorescence and by measuring the percentage of GFP negative cells, respectively, as described in Arroyo-Berdugo et al. (2023) and Di Mambro et al. (2023).

2.6 | Western blot

After harvest, cells were spun down for 5 min at 500 g, 4°C, washed with cold 1X TRIS buffer saline (TBS) and spun down again for 5 min at 500 g, 4°C. The pellets were lysed by sonication in radioimmunoprecipitation assay buffer (RIPA) buffer supplemented with protease inhibitors (10 μg ml^{-1} of aprotinin, leupeptin, antipain, soybean inhibitor and 1 mM phenylmehylsulfony fluoride [PMSF]) and phosphatase inhibitors (50 mM sodium fluoride, 1 mM sodium orthovanadate) (Protease inhibitors are from Sigma–Merck). The lysate was centrifuged at 2000 g for 5 min at 4°C to remove the insoluble material. The extract was collected and assayed in triplicate for protein quantification using the bicinchoninic acid (BCA) kit (Bio-Rad). The protein concentration was then determined by interpolation on a nine serial dilutions bovine serum albumin (BSA) standard curve generated in the same radioimmunoprecipitation assay buffer (RIPA) buffer within the concentration range of 0.1 to 2 mg ml^{-1}. Lysates were heated to 95°C in sodium dodecyl sulphate (SDS) sample buffer supplemented with 100 mM dTT for 5 min, separated by sodium dodecyl sulphate polyacrylamide gel electrophoresis (SDS-PAGE) and transferred to PVDF membranes 0.2 μm pore size (Amersham™). Membranes were blocked in 5% non-fat dry milk in TBS + 0.1% Tween-20 probed with the indicated antibodies (Tables S5 and S6), and reactive bands were visualised using ECL Prime (Pierce), according to the manufacturer's instructions. Band densities detection was obtained using Odyssey ® Fc Imaging System, LI-COR Biosciences. The Immunorelated procedures used comply with the recommendations made by the *British Journal of Pharmacology* (Alexander et al., 2018).

2.7 | RT-qPCR

RNA extraction and quantitative real-time polymerase chain reaction (RT-qPCR) were performed using the kit from Bioline and specific primers from Sigma–Merck (Haverill, UK), listed in Table S7. RT-qPCR was carried out using SensiFAST™ SYBR® No-ROX Kit (Bioline) (Bioline was distributed by SLS, Scientific Laboratory Supplies, Fairham, Nottingham UK), using the primers at a final concentration of 0.4 μM. The final concentration of cDNA used for each experiment was 20 ng. The reaction was conducted in The StepOnePlus™ Real Time System instrument (Applied Biosystem) with initial holding stage at 95 °C for 2 min, followed by 40 amplification cycles at 95°C (denaturation) for 30 s, 60°C (annealing) for 10 s and at 72°C (extension) for 20 s, with a single fluorescence measurement, and a final dissociation step (95°C for 30 s, 65°C for 30 s, 95°C for 30 s) and cooling holding at 4°C. To optimise

the RT-PCR conditions, the efficiency of the primers was determined using standard curve, generated from 1:10 dilution series of cDNA, from a calibrator cell line sample. glyceraldehyde 3-phosphate dehydrogenase (GAPDH) was used as housekeeping control for gene normalisation. The data were analysed by the Pfaffl equation.

2.8 | PP2A activity assay

PP2A activity was measured using the kit #17-313 from Sigma-Merck (Haverill, UK). Briefly, the cells were treated with okadaic acid, forskolin or combination and collected at specific timepoints, as described in the results. Cells were spun down at 500 g for 5 min at 4°C; pellets washed once with cold TBS 1× and centrifuged again for 5 min. The pellets were then lysed in PP2A activity lysis buffer (20 mM imidazole-HCl, 2 mM ethylenediaminetetraacetic acid (EDTA), 2 mM ethylene glycol tetraacetic acid (EGTA) pH 7.0 with 10 μg ml^{-1} each of aprotinin, leupeptin, soybean trypsin inhibitor, antipain, 1 mM benzamidine and 1 mM phenylmethylsulfonyl fluoride [PMSF]) and sonicated for 20 s. The lysates were then centrifuged at 2000 g for 5 min at 4°C. The concentration of proteins in the supernatants were determined by bicinchoninic acid (BCA) assay (Bio-Rad). For each assay, 200 μg of proteins was immunoprecipitated over night at 4°C with 4 μg of mouse anti-PP2A-c antibody (PP2A-c Merck 05-421, RRID AB_309726) or mouse anti PP2R2A antibody (Cell Signaling Technology #5689 RRID: AB_10827877) and 40 μg of protein A agarose in pNPP buffer in a final volume of 500 μl. The day after, the immunoprecipitates were washed three times with 700 μl of cold TBS 1×, followed by one wash with 500 μl pNPP buffer. The immunoprecipitates were centrifuged at 6000 rpm for 1 min at 4°C between each wash. After the last wash, the immunoprecipitated lysates was incubated with 20 μl pNPP buffer and 60 μl threonine phosphopeptide in agitation at 100 rpm for 20 min at 30°C. After the incubation period, the immunoprecipitated lysates were centrifuged at 6000 rpm for 1 min at 4°C. Twenty-five microlitres were transferred to a 96-well microtitre plate and incubated with 100 μl malachite AB solution. The absorbance was read at 650 nm, and the results were expressed as picomoles phosphate per microgram of protein used in the assay through a phosphate standard curve.

2.9 | Bioinformatic analysis

The gene expression profile of AML patients was obtained from Leucegene (GSE62190, GSE66917, GSE67039) (Lavallee et al., 2015). The data were analysed as described in Di Mambro et al. (2023).

2.10 | Analysis of intracellular daunorubicin by liquid chromatography-mass spectrometry (LC–MS)

Intracellular daunorubicin was measured on a Water TQSμ mass spectrometer, coupled to a Waters Acquity Ultra-High Performance Liquid Chromatography (UPLC) system. The UPLC was equipped with a Waters HSS T3 100Å 1.8 μm, 21 × 100 mm reverse phase column. Chromatographic separation was achieved using a binary gradient with solvent A water + 0.1% formic acid (*v*/*v*) and solvent B acetonitrile + 0.1% formic acid (*v*/*v*). The conditions were 1% B to 1 min, change to 40% B at 2 min, 60% B at 3 min and 95% B at 3.5 min, followed by re-equilibration at 1% for 1.5 min. Parameters for daunorubicin were optimised using direct injection, and daunorubicin was quantified by electrospray ionisation in positive mode using multiple reaction monitoring with transitions of 528 > 321 and 528 > 382, cone voltages of 15 V and collision energies of 21 and 8 eV, respectively. Data were quantified using a modified in-house work-flow based on Behrends et al. (2011).

2.11 | Molecular docking

System preparation: Cryo-EM structures of the human multidrug transporter, **ABCB1**, also known as P-glycoprotein (P-gp) or MDR1, were downloaded from the Protein Data Bank (https://www.rcsb.org/) (PDB IDs: 7A69 [ABCB1 with vincristine, resolution 3.20 Å] and 7A6F [ABCB1 with **zosuquidar**, resolution 3.50 Å]). The protein preparation tool in 'Flare v7.2, Cresset software' (https://www.cresset-group.com/software/flare/) (Flare, 2024) was utilised to correct any structural inconsistencies in the downloaded proteins and to optimise the hydrogen bonding network. Protonation states of amino acid residues were adjusted to reflect the physiological pH before the docking experiments.

A selection of three ligands targeting ABCB1 were sourced and downloaded from the PubChem database (https://pubchem.ncbi.nlm.nih.gov). The ligands are distinguished as either *substrates* (daunorubicin), compounds that are transported by P-gp across the cell membrane and released extracellularly, or *modulators* (1,9-dideoxyforskolin, forskolin), compounds that block the transport of substrates by competitive or noncompetitive binding to P-gp (Choi, 2005; Kim, 2002; Morris et al., 1991; Y. H. Wang et al., 2005; Zeino et al., 2014). Each compound was prepared using Flare's integrated ligand preparation tool (Flare, 2024) to achieve stable conformations and apply appropriate charges.

2.12 | Docking protocol

Molecular docking was performed using Flare (2024) for the three compounds bound to the two P-gp structures. The generated grid for the binding site was defined by the resolved ligand in each protein, **vincristine** (P-gp_v) and zosuquidar (P-gp_z) (Figure 6). Re-docking was performed to validate the molecular docking protocol using the 'Very accurate but slow' mode. Subsequently, all three compounds were docked in P-gp_v and P-gp_z.

2.13 | Molecular dynamics (MD) simulations

The CHARMM-GUI (Jo et al., 2008; Jo et al., 2009) membrane builder module was used to construct two protein complexes: P-gp_z

with daunorubicin and forskolin and P-gp$_z$ with daunorubicin and 1,9-dideoxyforskolin in a biologically relevant membrane system. Each protein complex was placed in a POPC:cholesterol (70:30) bilayer which has been explored previously (Thangapandian et al., 2020) (Figure 6). Each system was solvated neutralised with K^+ and Cl^- ions to achieve a net ionic concentration of 150 mM. Each system contained ~340,000 atoms with dimensions of 150 × 150 × 180 Å3 before any simulations. A multistep equilibration protocol was performed with the NAMD software, version 2.14 (Phillips et al., 2005), to remove close contacts in the structure. The backbones were initially fixed and then harmonically constrained, and water was restrained by small forces from penetrating the protein-lipid interface. The constraints on the protein were released gradually in three steps of 300 ps each, changing the force constants from 1 to 0.5 and 0.1 kcal/(mol Å2), respectively, with a time step of 1 fs. This was then followed by an unbiased MD simulation performed with a 2 fs integration time step and under constant temperature (310 K) maintained with Langevin dynamics, and 1 atmosphere constant pressure achieved by using the hybrid Nosé–Hoover Langevin piston method on a flexible periodic cell to capture long-range effects.

2.14 | Statistical analysis

The data and statistical analysis reported in this study comply with the recommendations set by the *British Journal of Pharmacology* on experimental design and analysis (Curtis et al., 2025). Data are expressed as mean ± standard deviation (SD) obtained from the indicated number (*n*) of individual samples and experiments. The data present the results of at least three independent experiments using group of similar size; for each experiment, we performed technical replicates (two or three technical replicates per experiment). Outliers were included in the data analysis and presentation. For some experiments, we were unable to repeat the experiments five times, which might represent a limitation of our study. Statistical analysis was carried out only where n was equal to or greater than 5. Randomisation and blinded analyses were conducted for some experiments to verify the validity of our results. This approach was not possible for all the experiments, and it might represent a limitation of our study. Statistical analyses were conducted using GraphPad Prism 10.2 (GraphPad software, CA). Statistical significance was considered at a *P*-value less than 0.05 for all the statistical tests used in the study, in compliance with Curtis et al. (2025). One asterisk appears in the figures where the results indicate statistical significance. Statistical significance was determined by using different statistical tests. When comparing means from more than two groups, two-way analysis of variance (ANOVA) was performed. Multiple comparison tests (post hoc) analyses were performed only if F was significant ($P < 0.05$), and there was no variance inhomogeneity for the groups. The data were normalised for controlling unwanted sources of variation, setting controls as 100% or 1 for comparison purposes and data analysed by non-parametric statistics, including two tailed student's *t*-test and one-way ANOVA.

2.15 | Nomenclature of targets and ligands

Key protein targets and ligands are hyperlinked to corresponding entries in http://www.guidetopharmacology.org and are archived in the Concise Guide to Pharmacology 2021/2022 (Alexander et al., 2023a,2023b).

3 | REAGENTS

Forskolin and **Daunorubicin** were purchased from Selleckchem (distributed by Stratech, Ely, UK). PKA inhibitors **KT5720** and **1,9 dideoxyforskolin** were purchased from Sigma–Merck (Haverill, UK). The antibodies used in this study are listed in Tables S5 and S6.

4 | RESULTS

4.1 | PP2A catalytic subunits are expressed in KMT2A-r AML cell lines and patients' cells

We analysed the expression of genes encoding for PP2A catalytic (*PPP2CA* and *PPP2CB*), structural (*PPP2R1A* and *PPP2R1B*) and regulatory subunits (*PPP2R2A*, *PPP2R2B*, *PPP2R2C*, *PPP2R2D PPP2R3A*, *PPP2R3B*, *PPP2R5A*, *PPP2R5B*, *PPP2R5C*, *PPP2R5D*, *PPP2R5E*, *STRN*, *STRN3* and *STRN4*) in a large RNA-seq dataset comprising *KMT2A*-r and *KMT2A*-wt- AML patients (Lavallee et al., 2015) (Figures 1a and S1). For *PPP2CA*, encoding for the catalytic subunit α (PP2A-Cα), the lowest expression of *PPP2CA* was found in complex karyotype AML and the highest expression in t(8;21)-AML (*KMT2A*-r vs AML with complex karyotype log 2 fold change = 0.419856; padj = 0.00216) (*KMT2A*-r vs AML with complex t (8;21) log 2 fold change = −0.4180; padj = 0.042641). For *PPP2CB*, encoding for PP2A-Cβ, the highest expression was found in trisomy/tetrasomy 8-AML, followed by *t* (15;17)-AML and complex karyotype AML (*KMT2A*-r vs AML with complex karyotype log 2 fold change = −0.53551; padj = 6.93E-06), (*KMT2A*-r vs AML with trisomy/tetrasomy of chromosome 8 log 2 fold change = −0.72147; padj = 0.000244) (*KMT2A*-r vs AML with *t* [15;17] log 2 fold change = −0.71338; padj = 0.000101). We then investigated the expression of *PPP2CA* and *PPP2CB* by RT-qPCR in *KMT2A*-r primary samples (P), *KMT2A*-r cell lines, *KMT2A*-wt cell lines and mononuclear cells isolated from bone marrow (BM) or peripheral blood (PB) isolated from healthy adult volunteers. We found no significant difference in *PPP2CA* expression between *KMT2A*-r primary samples and BM or PB controls (Figure 1b), whereas *PPP2CB* expression lower in *KMT2A*-r primary samples than in BM controls (Figure 1c). *PPP2CA* expression was higher in *KMT2A*-wt and *KMT2A*-r human cell lines than in the BM controls (Figure 1d), whereas there was no difference in the mRNA expression level of *PPP2CB* (Figure 1e). We then investigated the expression of PP2A-C in the same samples by Western blot (PP2A-c Merck 05-421, RRID: AB_309726; GAPDH Cell Signaling Technology 2118; RRID: AB_561053). The results revealed no differences among the *KMT2A*-r primary

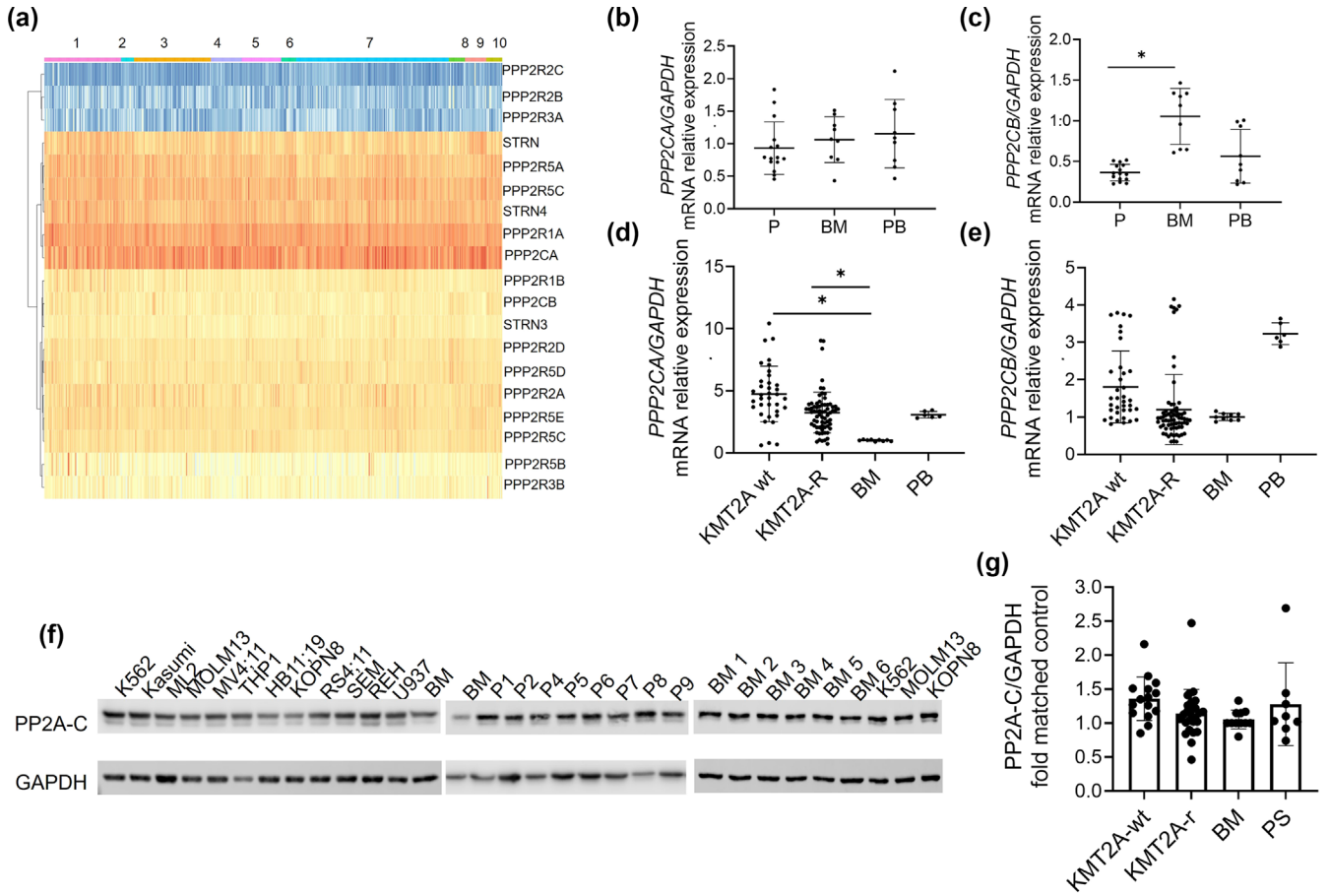

FIGURE 1 PP2A network gene expression in acute myeloid leukaemia (AML). (a) Heatmap of PP2A network *mRNA* in a large AML- RNA-seq dataset ($n = 384$) comprising 31 samples from patients carrying rearrangements of *KMT2A*. Meta-analyses of RNA-seq data from Leucegene (GSE62190, GSE66917, GSE67039). 1: complex karyotype, 2: EVI-r; 3: intermediate; 4: inversion 16; 5: *KMT2A*-r; 6: monosomy 5; 7 normal karyotype; 8: t(15:17); 9: t(8;21); 10 trisomy-tetrasomy 8. (b–e) qRT-PCR showing the expression of *PPP2CA* (b,d) and *PPP2CB* (c,e) in KMT2A-r patients (*P*) ($n = 5$), bone marrow isolated from health volunteers (BM) ($n = 3$), mononuclear cells isolated from peripheral blood of healthy volunteers (PB) ($n = 3$), KMT2A wild type (wt) ($n = 4$) and KMT2A rearranged (KMT2A-r) ($n = 9$) leukaemic cell lines. Gene expression was normalised to *GAPDH* control and analysed by Pfaffl equation. Values are expressed relative to BM controls. Data represent mean ± SD. As n was <5 for these experiments, statistical analysis was not carried out, and results should be regarded as preliminary.(f) Immunoblot of PP2A catalytic subunit (PP2Ac) in *KMT2A*-r AML cell lines (ML2, MOLM13, MV411, THP1), *KMT2A*-r ALL cell lines (HB11;19, KOPN8, RS4;11, SEM), *KMT2A*-r primary samples (P) and six independent healthy bone marrow (BM) controls. The data also present the expression of PP2Ac in four *KMT2A*-wt cell lines K562 (*BCR::ABL* (t19;22) erythroleukaemia cell line), Kasumi1 (*AML1:ETO, t8;21* AML cell line) REH (*TEL::AML1* [t12;21] ALL cell line) and U937 (*CALM::AF10*, AML cell line). GAPDH was used as a loading control. Densitometry analysis was conducted by LI-COR Image Studio software (g) Quantification of the densitometry analysis of PP2A. Values are expressed relative to BM controls.

samples or cell lines and the BM controls (Figure 1f–g). This result was consistent among several independent BM controls analysed. Collectively, these data indicate that the PP2A catalytic subunit is abundantly expressed in *KMT2A*-r AML patients and healthy BM controls.

4.2 | Forskolin arrests the proliferation and induces apoptosis in AML cells

Forskolin is a natural diterpene produced by the roots of the Indian plant *Coleus forskohlii* used for centuries in traditional medicine (Kanne et al., 2015; Sapio et al., 2017) and reported as a PP2A activator (Cristobal et al., 2011; Cristóbal et al., 2014; Feschenko et al., 2002; Neviani et al., 2005). We tested the effect of forskolin on the proliferation of four independent human leukaemic cell lines: two *KMT2A-wt* cell lines, Kasumi1 and K562, and two *KMT2A-r* AML cell lines, THP1 and MV411. As in our model, the cells stably express enhanced green fluorescent protein (eGFP) and the GFP fluorescence is proportional to the number of cells (Arroyo-Berdugo et al., 2023; Di Mambro et al., 2023); this biomarker was used as a reporter of cell viability. In eGFP-K562, forskolin had a detrimental effect on proliferation only at concentrations above 80 μM ($P < 0.0001$) (Figure 2a), whereas in the AML cell line eGFP-Kasumi1, this effect was observed at lower

concentrations (40 μM) ($P < 0.0001$) (Figure 2b). The cytostatic effect was even stronger in the *KMT2A*-r AML cell lines eGFP-THP1 and eGFP-MV411, as their proliferation was inhibited with a concentration of forskolin of 10 μM ($P < 0.0001$) (Figure 2c,d). We then investigated whether forskolin induced apoptosis by analysing, by flow cytometry, the percentage of GFP negative (GFP−) cells (Arroyo-Berdugo et al., 2023; Di Mambro et al., 2023). Forskolin induced an increase in the percentage of apoptotic cells only at concentrations above 150 μM in eGFP-K562 (Figure 2e) and above 80 μM in eGFP-Kasumi1 (Figure 2f). In the *KMT2A*-r AML cell lines, the effect was concentration dependent with a increase in the percentage of apoptotic cells with concentrations above 40 μM (Figures 2g and h and S2). These data indicate that forskolin has a cytostatic and cytotoxic effect on leukaemic cell lines.

4.3 | Forskolin increases the response of *KMT2A*-r cells to daunorubicin

Previous studies have reported that forskolin increases the response of cancer cells to chemotherapeutic agents (Cristobal et al., 2011; Illiano, Sapio, et al., 2018). We therefore investigated whether forskolin could enhance **daunorubicin**-induced cytotoxicity in AML cells. To this aim, we tested 40 μM forskolin, a concentration that had been shown to activate PP2A in vitro with no cytotoxic effects on healthy BM mononuclear cells (Neviani et al., 2005), in combination with 10 nM daunorubicin, a concentration that had very little effect on proliferation and viability of *KMT2A*-wt and *KMT2A*-r AML cells (Figure S3). Whereas the combination of forskolin and daunorubicin did not induce a statistically significant effect in eGFP-Kasumi1 (Figure 3b), forskolin significantly increased the response to daunorubicin in eGFP-K562 and in the *KMT2A*-r cell lines (Figures 3a–d and S4). As the BM microenvironment mediates resistance to chemotherapy (Arroyo-Berdugo et al., 2023), we evaluated the effect of the individual drugs and of their combination on *KMT2A*-r cell lines co-cultured with the human bone marrow stromal cell (BMSC) line HS5. The stroma decreased the response of eGFP-MV411 to forskolin, whereas the effect was not significant for eGFP-THP1 (Figure 3e and f). For the combination treatment, the results showed a decrease in the cytotoxic effect for both *KMT2A*-r cell lines when they were co-cultured with HS5 (Figures 3e and f and S5). To evaluate the potential impact of such a combination regimen in *KMT2A*-r leukaemia, we tested it in two *KMT2A*-r patient-derived xenograft (PDX) models by in vitro colony assay. Whereas the single treatment with either daunorubicin or forskolin had a modest impact, the combination treatment impaired the formation of colonies (Figure 3g and h). These

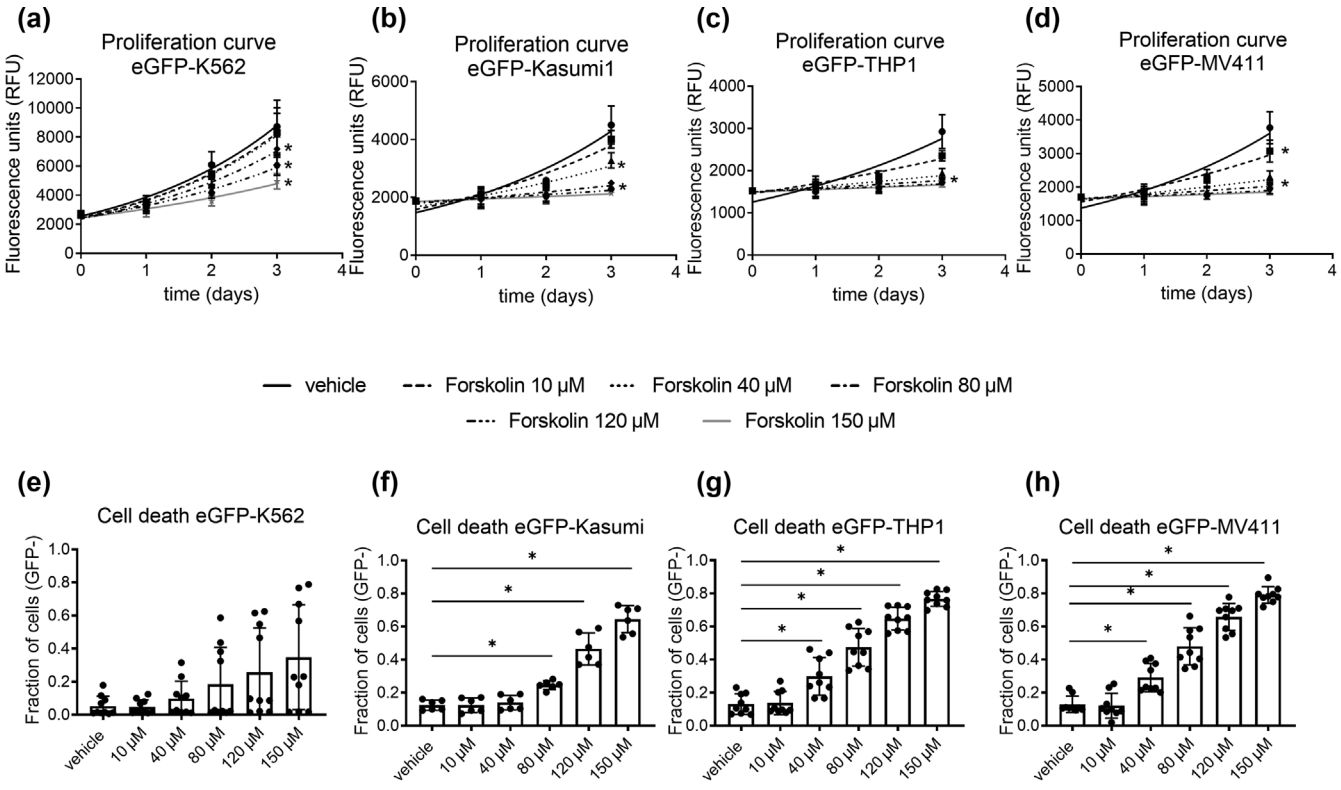

FIGURE 2 Forskolin has a cytostatic and cytotoxic effect on leukaemic cells. (a–d) Proliferation curve of eGFP-K562, eGFP-Kasumi1, eGFP-THP1 and eGFP-MV411 upon treatment with forskolin for 3 days. GFP expression was used as quantitative reporter of cell proliferation. For each cell line, the same number of cells was plated at t0, and the GFP signal was measured with a fluorescent microplate reader every 2 days. Data show mean ± SD of triplicate wells and three independent experiments. (e–h) Fraction of GFP-cells undergoing cell death upon forskolin treatment for 72 hours. Data show mean ± SD of triplicate wells and three independent experiments. As n was <5 for these experiments, results should be regarded as preliminary.

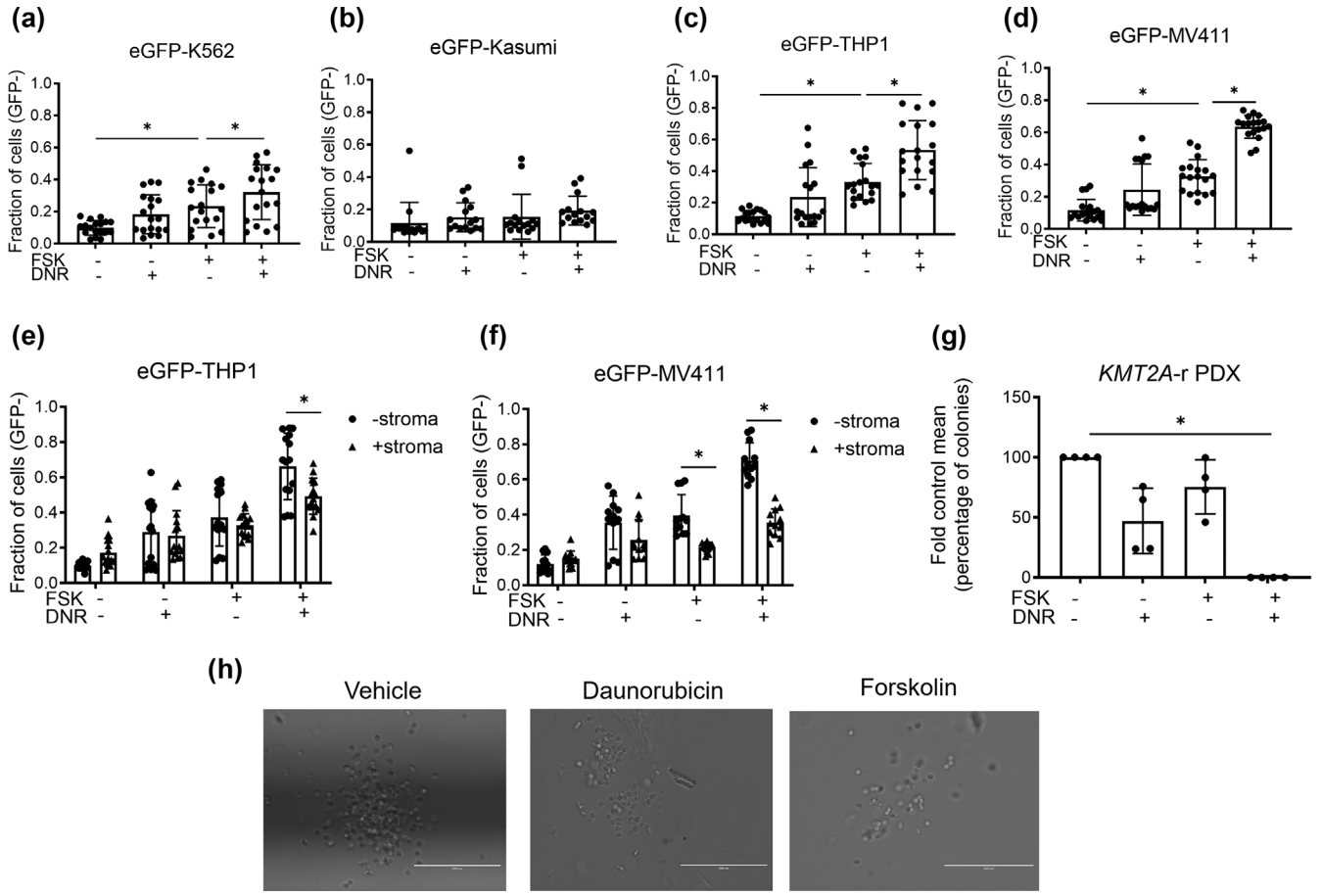

FIGURE 3 Combination of forskolin with daunorubicin in *KMT2A*-r leukaemic cells. (a–d) Analysis of cell death. Cells were treated with 40 μM forskolin, 10 nM daunorubicin or combination for 72 h. The GFP signal was used as quantitative reporter of alive, non-dead cells and measured by flow cytometry. Data show mean ± SD of triplicate wells for six (a, c, d) and five (b) independent experiments. Two-way ANOVA Tukey's multiple comparison test. (e–f) Effect of bone marrow stroma on forskolin–daunorubicin cytotoxicity. Cells were grown with or without stroma and treated with 40 μM forskolin, 10 nM daunorubicin or combination for 72 h. GFP signal was used as quantitative reporter of alive, non-dead cells and measured by flow cytometry. Data show mean ± SD of triplicate wells for four independent experiments. (g) Effect of 40 μM forskolin, 10 nM daunorubicin or combination on colony-forming unit ability of *KMT2A*-r patient-derived xenotransplant (PDX) samples. Data show the percentage of colonies in comparison to vehicle treated cells and the mean ± SD of duplicate wells and are representative of two independent samples. Where n <5, statistical analysis was not carried out, and results should be regarded as preliminary. (h) Colony morphology of *KMT2A*-r PDX. Cells were treated with the drugs in MethoCult for 14 days. Digital microscope images were captured using Evos FL digital inverted fluorescence microscope (magnification 40X).

data indicated that forskolin increases the response of *KMT2A*-r AML cells and PDX to daunorubicin and that stromal cells mediate resistance to this treatment.

4.4 | Forskolin activates PP2A, inhibits ERK1/2 and decreases the expression of c-MYC

To investigate whether the observed effects of forskolin were because of the activation of PP2A, we first analysed the phosphorylation of PP2A targeted pathways by Western blot, 48 h after treatment with forskolin (phosphor ERK1/2 Cell Signaling Technology 9101, RRID: AB_331646; ERK1/2 Santacruz sc514302, RRID: AB_2571739; phosphoAKT-Ser 473 Cell Signaling Technology 5060, RRID: AB_2315049; pan-AKT Cell Signaling Technology 4691; RRID: 915783; phosphoGSK3β Ser9 Cell Signaling Technology 5558; RRID: AB_10013750; GSK3β Cell Signaling technology 9832 RRID: AB_10839406). We observed a statistically significant decrease in the levels of phospho-**ERK1/2** (Thr202/Tyr204) in all the cell lines analysed, whereas we did not observe statistically significant changes in phospho-**AKT1** (Ser473) and phospho-**GSK3β** (Ser9) (Figure 4a–d). As c-MYC is a critical substrate of PP2A complex in cancer (Di Mambro et al., 2023; Goswami et al., 2022; Pippa & Odero, 2020; Yeh et al., 2004) and a critical mediator of proliferative metabolism in *KMT2A*-r leukaemia (Miyamoto et al., 2021), we evaluated the effect of forskolin on the expression of c-MYC (Cell Signaling Technology 9402S RRID:AB_2151827). We observed a decrease in c-MYC in *KMT2A*-r AML lines upon forskolin treatment (Figure 4a and e). To investigate whether this effect was because of repression of transcriptional expression, we evaluated the expression of c-*MYC* by RT-

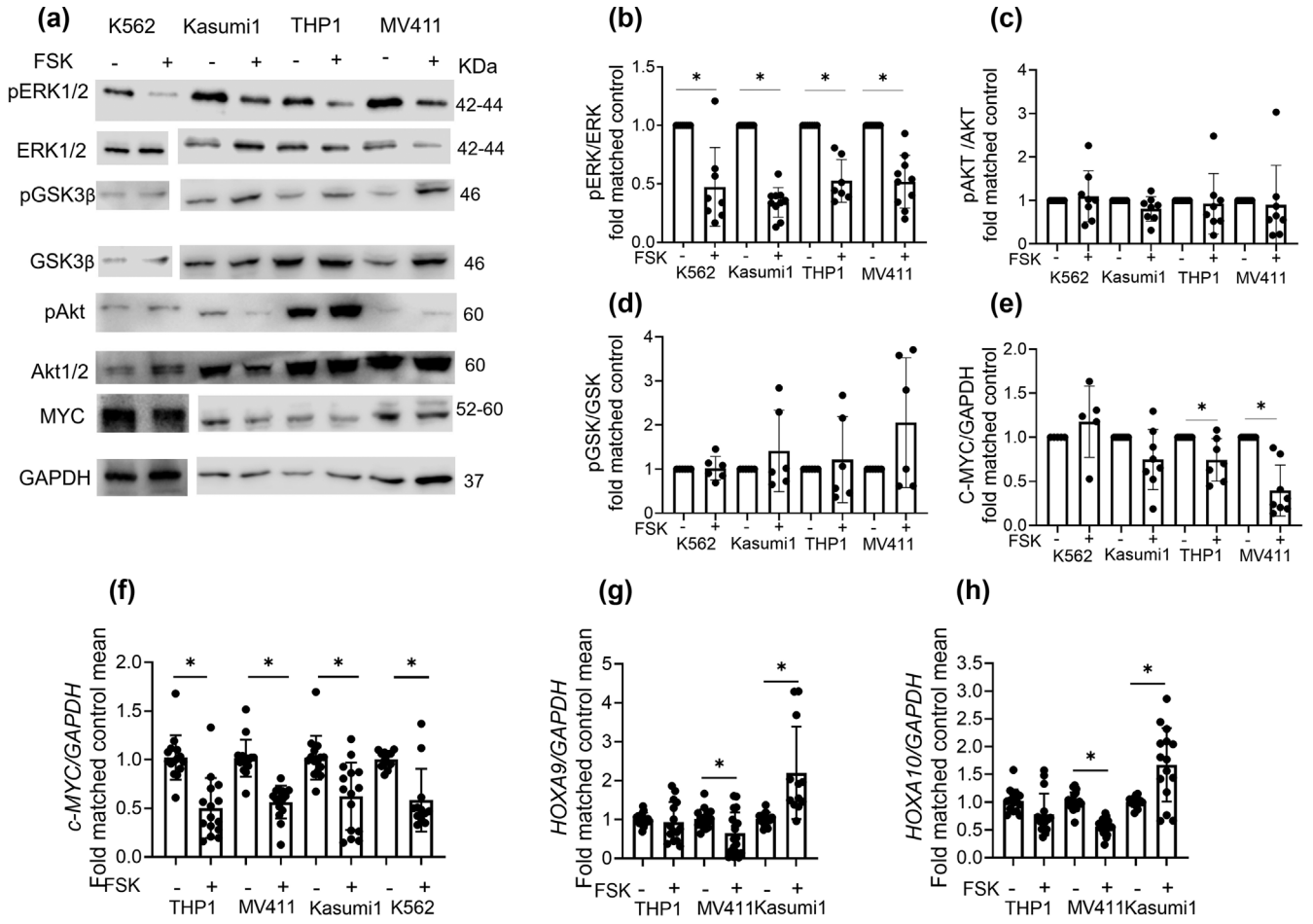

FIGURE 4 Effect of forskolin on PP2A downstream signalling pathways. (a) Immunoblot for phospho-AKT1/2 (Ser473) (60 KDa), AKT1/2 (pan)(60 KDa), phosphoGSK3β (Ser9) (46 KDa), GSK3β (46 KDa), phosphoERK1/2 (Thr202/Tyr204) (42–44 KDa), ERK1/2 (42–44 KDa), MYC (60 KDa) and GAPDH (37 KDa) in K562, Kasumi1, THP1 and MV411 upon 40 μM forskolin treatment for 48 h. Densitometry analysis was conducted by LI-COR Image Studio software. GAPDH was used as a loading control. (b–e) Quantification of the densitometry analysis of pERK1/2, normalised by ERK1/2, pAKT1/2, normalised by Akt1/2, pGS3Kβ, normalised by GSK3β and c-MYC, normalised by GAPDH. Data represent mean ± SD; values are expressed relative to vehicle controls. For the graph B, the data represent the results of four to five experiments and two technical replicas. For the graph C, the data represent the results of four experiments and two technical replicas. For the graph D, the data represent the results of three experiments and two technical replicas. For the graph E, the data represent the results of four to five independent experiments and two technical replicas. The data were analysed by non-parametric Wilcoxon matched pairs signed rank test. (f–h) RT-qPCR showing the expression of c-*MYC*, *HOXA9* and *HOXA10* in leukaemic cell lines upon forskolin treatment for 48 h. Gene expression was normalised against *GAPDH* control and analysed by Pfaffl equation. Values are expressed relative to vehicle controls. Data represent mean ± SD of three technical replicas and four to five independent experiments. The data were analysed by non-parametric Wilcoxon matched pairs signed rank test. Wherever n was <5, statistical analysis was not carried out, and results should be regarded as preliminary.

qPCR. The data indicated that forskolin had a repressive effect on the expression of c-*MYC* in all the cell lines analysed (Figure 4f). In addition, in the *KMT2A*-r cell line MV411, forskolin decreased the KMT2A target genes *HOXA9* and *HOXA10*, whereas it increased their expression in AML *KMT2A*-wt cell line Kasumi1 (Figure 4g and h). *HOXA9* and *HOXA10* were not detected in K562.

To understand whether the cytotoxic effect of forskolin on *KMT2A*-r cells was dependent on PP2A activation, we determined the activity of PP2A in cell treated with forskolin alone or pre-treated with the phosphatase inhibitor **okadaic acid** (OA) for 4 h, prior to forskolin. OA is an inhibitor of PP2A (IC50 0.1 nM) and **PP1** (IC50 10–15 nM) (Xing et al., 2006); for the combination experiments, we used 2.5 nM OA, a concentration that inhibits preferentially PP2A, as determined by analysis of PP2A activity and by analysis of PP2A phospho-targets (Figures 5a and S6A–E). These results were not affected by the level of PP2A-C that did not change upon OA treatment (Figure S6B). We then determined the impact of forskolin alone, or after pre-treatment with 2.5 nM OA for 4 h, on the enzymatic activity of PP2A. Forskolin increased the activity of PP2A (Figure S6F), despite the levels of PP2A-C were decreased upon forskolin treatment (Figure 5b and c). We normalised the activity of PP2A for the expression of PP2A-C; the results

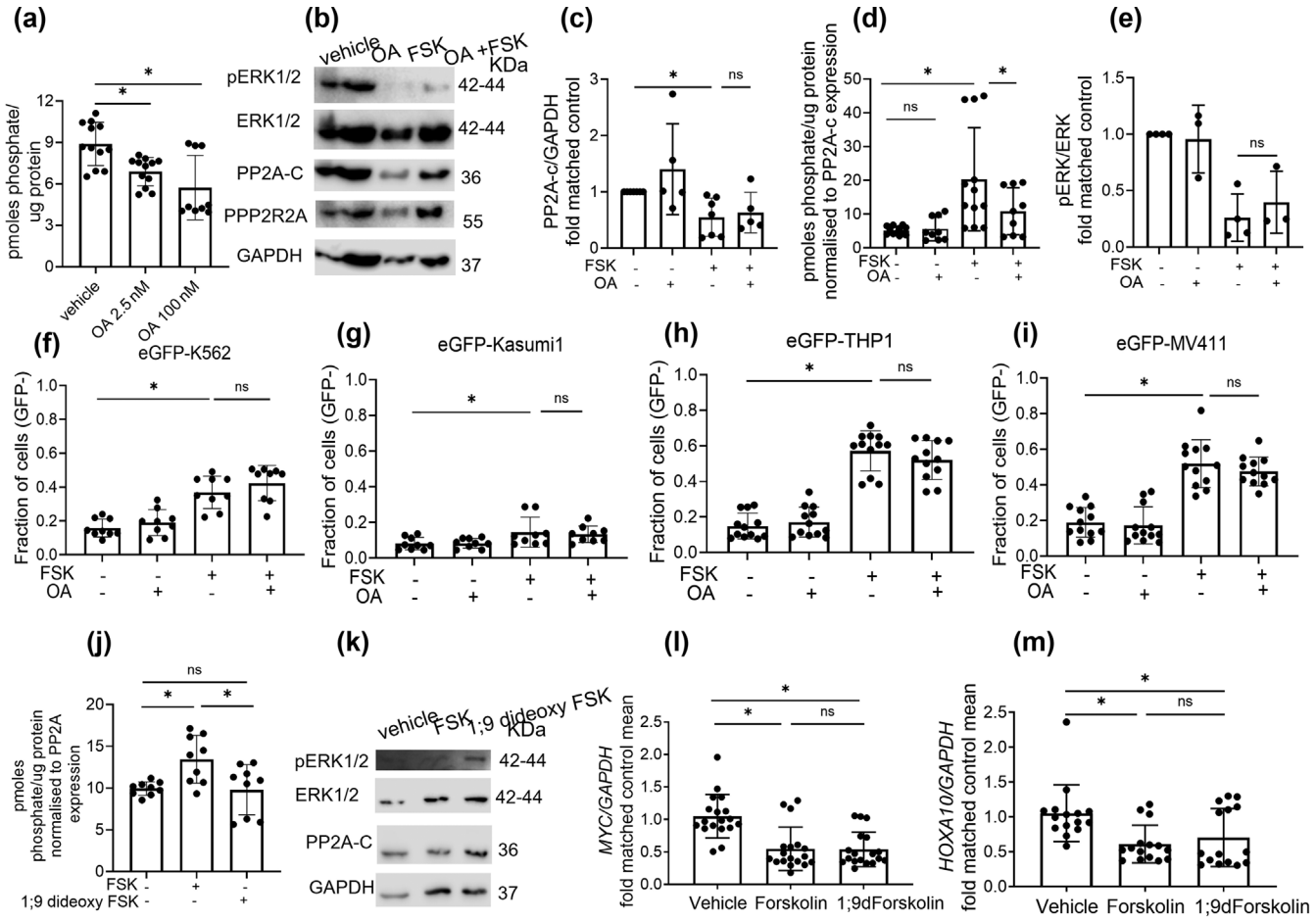

FIGURE 5 Effect of forskolin and 1;9 dideoxyforskolin on PP2A activity and gene expression. (a) PP2A enzymatic activity assay analysed in MV411 treated with okadaic acid for 4 h. Data show mean ± SD of three technical replicas and three to four independent experiments. Two-way ANOVA Sidak's multiple comparison test. (b) Immunoblot for phosphoERK1/2 (Thr202/Tyr204) (42–44 KDa), ERK1/2 (42-44KDa), PP2A-c (36 KDa), PP2R2A (55 KDa) and GAPDH (37 KDa) in MV411 pre-treated for 4 h with okadaic acid 2.5 nM, followed by forskolin 40 μM for additional 48 h. Densitometry analysis was conducted by LI-COR Image Studio software. GAPDH was used as a loading control. (c) Quantification of the densitometry analysis of PP2A-c, normalised by the levels of GAPDH. The data show mean ± SD of two technical replicas of three to four independent experiments. (d) PP2A enzymatic activity assay analysed in MV411 pre-treated with okadaic acid 2.5 nM for 4 h, followed by forskolin 40 μM for 48 h. Data show mean ± SD of three technical replicas of three to four independent experiments. (e) Quantification of the densitometry analysis of pERK1/2, normalised by the levels of ERK1/2. The data show mean ± SD of three to four independent experiments. (f-i) Analysis of cell death upon forskolin treatment. Cells were pre-treated with 2.5 nM okadaic acid for 4 h and then treated with 40 μM forskolin for 72 h. GFP signal was used as quantitative reporter of alive, non-dead cells and measured by flow cytometry. Data show mean ± SD of three technical replicas and three independent experiments.. (j) PP2A enzymatic activity assay analysed in MV411 treated with forskolin or 1;9 dideoxyforskolin 40 μM for 48 h. Data show mean ± SD of three technical replicas for three independent experiments. (k) Immunoblot for phosphoERK1/2 (Thr202/Tyr204) (42–44 KDa), ERK1/2 (42–44 KDa), PP2A-C (36 KDa), PP2R2A (55KDa) and GAPDH (37 KDa) in MV411 treated with forskolin or 1;9 dideoxyforskolin 40 μM for 48 h. Densitometry analysis was conducted by LI-COR Image Studio software. GAPDH was used as a loading control. (l–m) qRT-PCR showing the expression of c-*MYC* and *HOXA10* in eGFP-MV411 upon forskolin and 1;9 diseoxyforskolin treatment for 48 h. Gene expression was normalised by *GAPDH* control and analysed by Pfaffl equation. Values are expressed relative to vehicle controls. Data represent mean ± SD of triplicate wells and four independent experiments. As n was <5 for these experiments, statistical analysis was not carried out, and results should be regarded as preliminary.

confirmed that forskolin increased the activity of PP2A (Figure 5d); these results were also confirmed when PP2A activity was measured in protein lysates immunoprecipitated with a distinct antibody against the regulatory subunit PPP2R2A, and the data normalised by PPP2R2A expression (Figure S6G and H). Notably, the activity of PP2A in cells pre-treated with OA, prior to forskolin treatment, was lower than in those treated with forskolin alone (Figure 5d). Despite this difference, there was no significant difference in pERK/ERK1/2 ratio between the cells treated with forskolin alone and those pre-treated with okadaic acid prior to forskolin (Figure 5b and e). Consistent with these data, both forskolin and the combination of forskolin and OA increased the percentage of dead cells, with no

statistically significant difference between the cellular outcomes in these conditions (Figures 5f,i and S7). These data demonstrate that forskolin activates PP2A and also suggest that forskolin might stimulate other phosphatases implicated in the dephosphorylation of residues Thr202/Tyr204 on ERK1/2.

Forskolin is a potent activator of **adenylate cyclase**, which stimulates the production of cAMP (Sapio et al., 2017). To understand the role of the stimulation of adenylate cyclase and cAMP in forskolin-mediated PP2A activation, we analysed the effect of 1,9-dideoxy-forskolin, a forskolin analogue that lacks adenylate cyclase activating function, on PP2A activity. Our results showed that 1,9-dideoxy-forskolin was not as potent as forskolin in stimulating PP2A activity (Figures 5j,k and S6 I,J), suggesting that the molecular mechanism underlying forskolin-mediated PP2A activation could be dependent on stimulation of adenylate cyclase and cAMP. As our data pointed to a repression of *c-MYC* and *HOXA10* transcription, we evaluated the effect of 1,9-dideoxy-forskolin on c-*MYC* and *HOXA10* by RT-qPCR in *KMT2A*-r cell line MV411. The data showed that both forskolin and 1,9-dideoxy-forskolin decreased the expression of these genes (Figure 5l and m). We also discovered that both forskolin and 1,9-dideoxy-forskolin had a suppressive effect on *PPP2CA* expression (Figure S6K). Overall, the data indicate that forskolin activates PP2A; stimulates dephosphorylation of ERK1/2; and represses the expression *c-MYC*, *HOXA10* and *PPP2CA*. These effects are not fully dependent on stimulation of adenylate cyclase and point to a non-canonical mechanism.

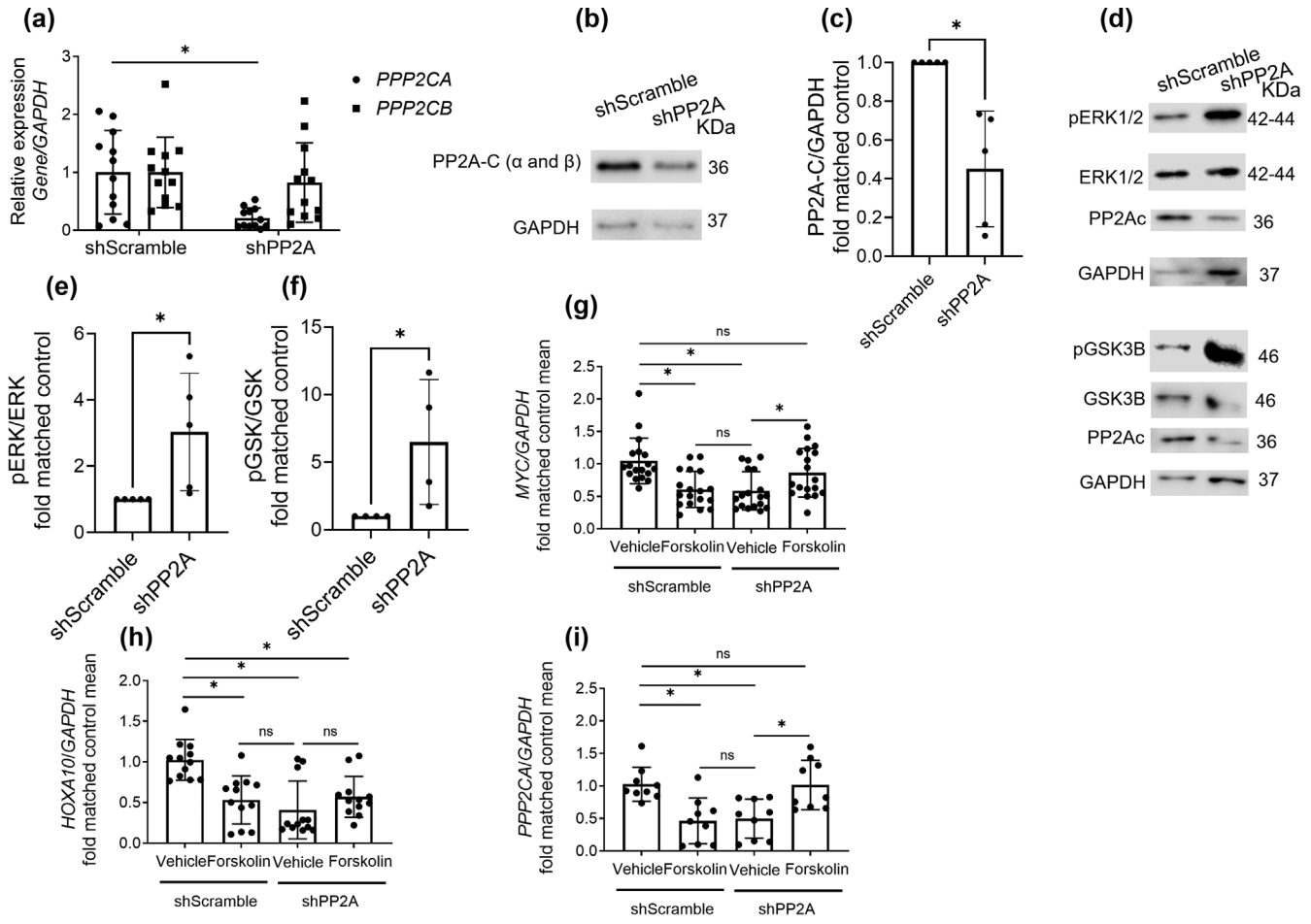

FIGURE 6 Effect of PPP2CA gene silencing on response to forskolin. (a) RT-qPCR showing the expression of *PPP2CA* and *PPP2CB* in eGFP-MV411 shPP2A. Gene expression was normalised by *GAPDH* control and analysed by Pfaffl equation. Values are expressed relative to shScramble controls. Data represent mean ± SD of triplicate wells and four independent experiments. (b) Immunoblot for PP2A-c (36 KDa) and GAPDH (37 KDa) in eGFP-MV411 transfected with either shScramble or shPP2A. GAPDH was used as a loading control. (c) Quantification of the densitometry analysis of PP2A-c, normalised by the levels of GAPDH. The data show mean ± SD of five independent experiments. Non-parametric Mann–Whitney test. (d) Immunoblot for phosphoGSK3β (Ser9) (42 KDa), GSK3β (42 KDa), phosphoERK1/2 (Thr202/Tyr204) (42–44 KDa), ERK1/2 (42–44 KDa) and GAPDH (37 KDa) in eGFP-MV411 transfected with either shScramble or shPP2A. GAPDH was used as a loading control. (e–f) Quantification of the densitometry analysis of pERK1/2 and pGSK3β normalised by the levels of GAPDH. The data show mean ± SD of five and four independent experiments. (g, h and i) RT-qPCR showing the expression of c-*MYC*, *HOXA10* and *PPP2CA* in eGFP-MV411 shScramble and shPP2A upon forskolin treatment for 48 h. Gene expression was normalised by *GAPDH* control and analysed by Pfaffl equation. Values are expressed relative to shScramble vehicle controls. Data represent mean ± SD of three technical replicates of five, four and three independent experiments. Wherever n was <5, statistical analysis was not carried out, and results should be regarded as preliminary.

4.5 | The inhibitory effect of forskolin on c-MYC expression is dependent on PP2A expression

To further investigate the role of PP2A in the molecular mechanism of forskolin, we generated an eMV411-GFP cell line where *PPP2CA* was silenced by RNA interference (Di Mambro et al., 2023). We confirmed the knockdown (KD) of *PPP2CA* in this cell line by RT-qPCR and Western blot (Figure 6a–c). Whereas the antibody used for the Western blot is unable to distinguish the α and β subunits of PP2A-C, the RT-qPCR enabled us to confirm the specific KD of

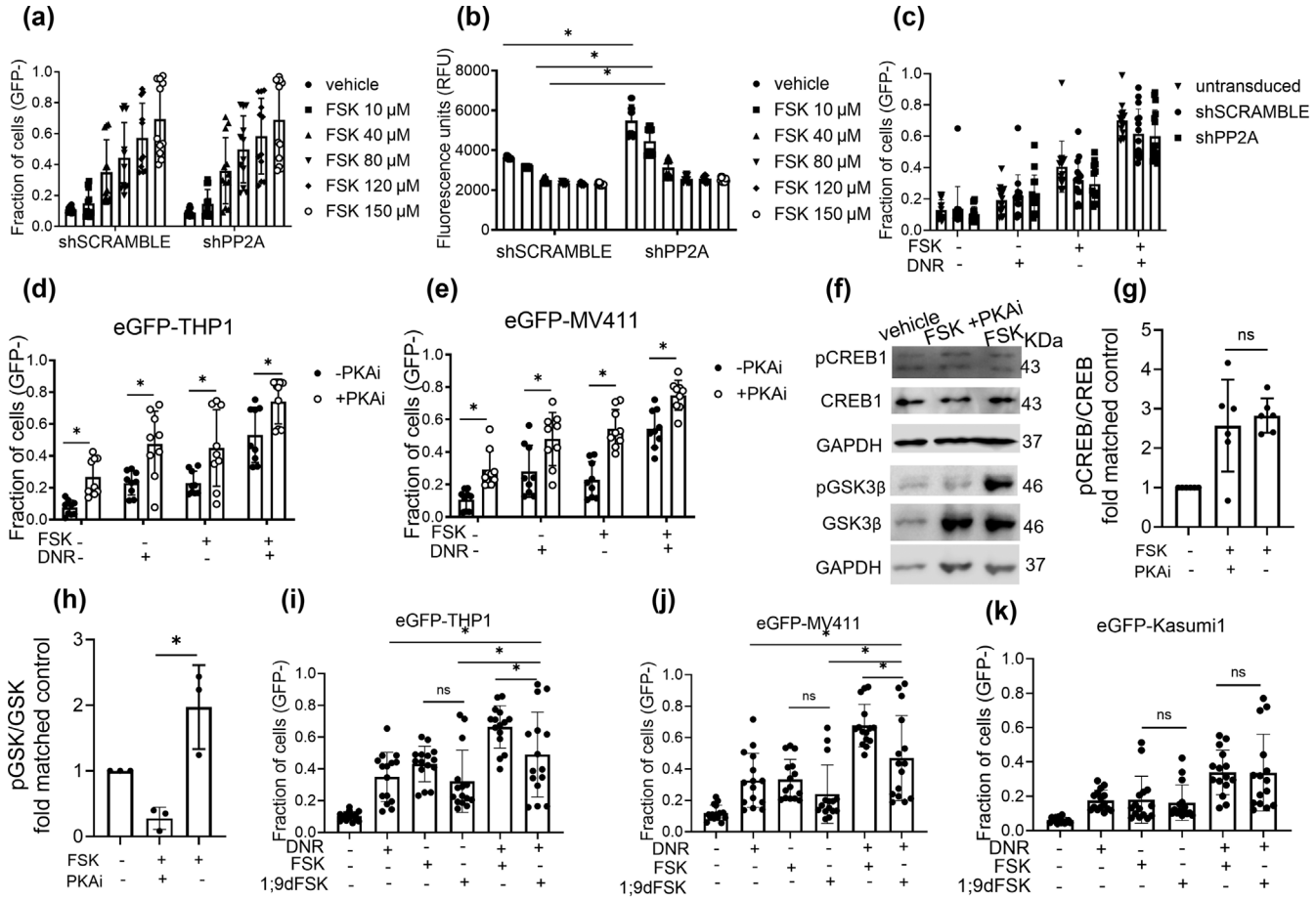

FIGURE 7 Effect of adenylate cyclase stimulation and PKA inhibition on forskolin-mediated daunorubicin potentisation. (a) Analysis of cell death of eGFP-MV411 shScramble and shPP2A upon forskolin treatment for 3 days. GFP signal was used as quantitative reporter of alive, non-apoptotic cells and measured by flow cytometry. Data show mean ± SD of triplicate wells and four independent experiments. (b) Analysis of proliferation of eGFP-MV411 shScramble and shPP2A upon forskolin treatment for 3 days. GFP expression was used as quantitative reporter of cell proliferation. For each cell line, the same number of cells was plated at t0, and the GFP signal was measured with a fluorescent microplate reader every 2 days. Data show mean ± SD of triplicate wells and four independent experiments. (c) Analysis of cell death in eGFP-MV411 shScramble and shPP2A upon forskolin and daunorubicin treatment. Cells were treated with 40 μM forskolin, 10 nM daunorubicin or combination for 72 h. GFP signal was used as quantitative reporter of alive, non-dead cells and measured by flow cytometry. Data show mean ± SD of triplicate wells and five independent experiments. Two-way ANOVA Sidak's multiple comparison test. (d and e) Effect of PKA inhibition on response to daunorubicin and forskolin. Analysis of cell death in eGFP-MV411 and THP1 upon forskolin and daunorubicin treatment. Cells were pre-treated with 10 μM PKA inhibitor or DMSO for 1-h prior incubation with 40 μM forskolin, 10 nM daunorubicin or combination for 72 h. GFP signal was used as quantitative reporter of alive, non-dead cells and measured by flow cytometry. Data show mean ± SD of triplicate wells and three independent experiments. (f) Immunoblot for phosphoCREB (Ser133) (43 KDa), CREB1 (43 KDa), pGSK3β (Ser9) (46 KDa), GSK3β (46 KDa) and GAPDH (37 KDa) in eGFP-MV411 pre-treated for 1 h with PKAi 10 μM, followed by forskolin 40 μM for 1 h. GAPDH was used as a loading control. (g) Quantification of the densitometry analysis of pCREB1, normalised by the levels of CREB1. The data show mean ± SD of technical duplicates of three independent experiments. (h) Quantification of the densitometry analysis of pGSK3β, normalised by the levels of GSK3β. The data show mean ± SD of three independent experiments. (i–k) Analysis is of cell death in eGFP- THP1, MV411 and Kasumi1 upon forskolin or 1;9 dideoxy forskolin treatment in combination with daunorubicin. Cells were treated with either 40 μM of forskolin or 1;9 dideoxyforskolin, 10 nM daunorubicin or combination for 72 h. GFP signal was used as quantitative reporter of alive, non-dead cells and measured by flow cytometry. Data show mean ± SD of triplicate wells and five independent experiments. Two-way ANOVA Tukey's multiple comparison test. Wherever n was <5, statistical analysis was not carried out, and results should be regarded as preliminary.

PPP2CA with no effect on *PPP2CB* expression. To characterise the impact of *PPP2CA* knockdown, we evaluated by Western blot the levels of phosphorylation of two PP2A targets, phospho-ERK1 (Thr202/Tyr204) and phospho-GSK3Bβ (Ser9). The data show that upon *PPP2CA* knockdown there is a statistically significant increase in the levels of phospho-ERK1 (Thr202/Tyr204) and phospho-GSK3Bβ (Ser9) (Figure 6d–f), highlighting the impact of PP2A on the phosphorylation of these residues, as reported in PhosphositePlus. We then evaluated the effect of forskolin on the expression of c-*MYC*, *HOXA10* and *PPP2CA* on this cell line. Whereas forskolin decreased the expression of c-*MYC*, *HOXA10* and *PPP2CA* in the parental scramble cell line, forskolin increased the expression of *c-MYC* and *PPP2CA* in the *PPP2CA* KD cell line (Figure 6g and h); there was no statistically significant difference in *HOXA10* expression between the *PPP2CA* KD cell line treated with vehicle and with forskolin (Figure 6a and h). Overall, these data indicated that the repressive effect of forskolin on *c-MYC* and *HOXA10* expression is dependent on PP2A expression/activation.

4.6 | The effect induced by combining forskolin and daunorubicin is not dependent on PP2A activation nor on adenylate cyclase stimulation

We then evaluated the impact of PP2A knockdown on the cytotoxic and cytostatic effects of forskolin. The data indicate no difference in the IC_{50} and in the percentage of dead cells between shScramble and shPP2A cells treated with increasing concentrations of forskolin (Figures 7a and S8). Concentrations of forskolin higher than 40 μM affected the proliferation of the two cell lines (shScramble and shPPP2CA) equally (Figures 7b and S8). To understand whether PP2A activation mediates the cytotoxic effect of the combination between forskolin and daunorubicin, we investigated the effect of this drug combination in eGFP-MV411-shPP2A. The results indicated no significant differences between shScramble and shPPP2CA cells (Figures 7c and S9), suggesting that the effect of the combination between forskolin and daunorubicin on *KMT2A*-r cells is not dependent on PP2A expression/activation.

We then investigated whether the observed cytotoxic effect of forskolin in combination with daunorubicin was dependent on stimulation of adenylate cyclase and activation of cAMP-dependent **Protein Kinase A (PKA)**. Pre-treatment with the 10-uM PKA inhibitor (PKAi) for 1 h prior forskolin and daunorubicin treatment did not rescue the leukaemic cells from the cytotoxic effect of forskolin, suggesting that the cytotoxic effect was not dependent on PKA activation (Figures 7d,e and S10). Pre-treatment with PKAi prior to forskolin did not affect the levels of phosphorylated CREB1 (Ser 133), a downstream target of PKA, whereas it decreased the levels of phosphorylated GSK3β (Ser9), another target of PKA (Fang et al., 2000) (phosphoCREB1 Ser133 Santacruz sc81486 RRID: AB_1125727; CREB1 Cell Signalling Technology 9197, RRID: AB_331277) (Figure 7f–h). These results indicate that PKAi antagonises the phosphorylation of GSK3β on Ser9 but does not affect the phosphorylation of CREB1 on Ser133, suggesting that additional kinases could contribute to the sustained levels of pCREB1 (Ser133) upon forskolin treatment. It is important to highlight that the antibody against pCREB1 (Ser133) also recognises pATF1 (Ser63), hence the two bands shown in the Western blot. We then analysed the effect of combining daunorubicin with 1,9-dideoxy-forskolin. Our results showed that 1,9-dideoxy-forskolin had a cytotoxic effect similar to forskolin and that there was no statistically significant difference in the outcome of these two drugs (Figures 7h,j and S11). 1,9-dideoxy-forskolin increased the response of *KMT2A*-r AML cells to daunorubicin, albeit it was less potent than forskolin, as indicated by the statistical analysis between the outcomes of forskolin + daunorubicin and 1,9-dideoxy-forskolin + daunorubicin. Overall, the data indicate that the ability of forskolin to potentiate the response to daunorubicin is not dependent on PP2A activation, nor stimulation of adenylate cyclase and cAMP increase.

4.7 | Forskolin potentiates the response to daunorubicin by inhibiting P-glycoprotein

Previous studies have suggested that forskolin and other diterpenes can bind and inhibit **P-glycoprotein** (P-gp), also known as ATP-dependent translocase ABCB1 or multidrug resistance protein (MDR), an energy dependent plasma membrane efflux pump that mediates the elimination of daunorubicin and other xenobiotics out of the cells (Morris et al., 1991; Morris et al., 1994; Safa, 2004). We therefore tested the effect of forskolin on efflux of daunorubicin by measuring the intracellular levels of daunorubicin by LC–MS. The data indicate that 1 h after treatment, there is a higher level of daunorubicin in MV411 cells treated with daunorubicin and forskolin than with daunorubicin alone (Figure 8a). These differences are non-significant at later time points (4 and 24 h). We docked forskolin, 1,9-dideoxyforskolin and daunorubicin (Figure 8b) to the structure of P-gp (Figure 8c) to uncover potential simultaneous occupancy and binding mechanisms. Our findings show a significant overlap in the binding site residues of forskolin or 1,9-dideoxyforskolin, indicating that both compounds bind to the same binding pocket of P-gp (Figure 8d). Moreover, there is a significant overlap for daunorubicin in both complexes, suggesting a shared interaction landscape that facilitates the concurrent accommodation of daunorubicin and forskolin (or 1,9-dideoxyforskolin) without steric hindrance (Figure 8d). Additionally, we extended the comparative analysis to a known substrate with established anti-cancer properties, **vincristine**, also characterised by electron microscopy (EM), bound to P-gp, (PDB ID: 7A69) (Nosol et al., 2020). Despite its larger and more globular structure, this substrate occupies the same binding site, underscoring the site's versatile accommodation capacity (Figure S12).

Collectively, these data indicate that forskolin increases the intracellular accumulation of daunorubicin and that this mechanism might be mediated by exerting an inhibitory effect on P-glycoprotein.

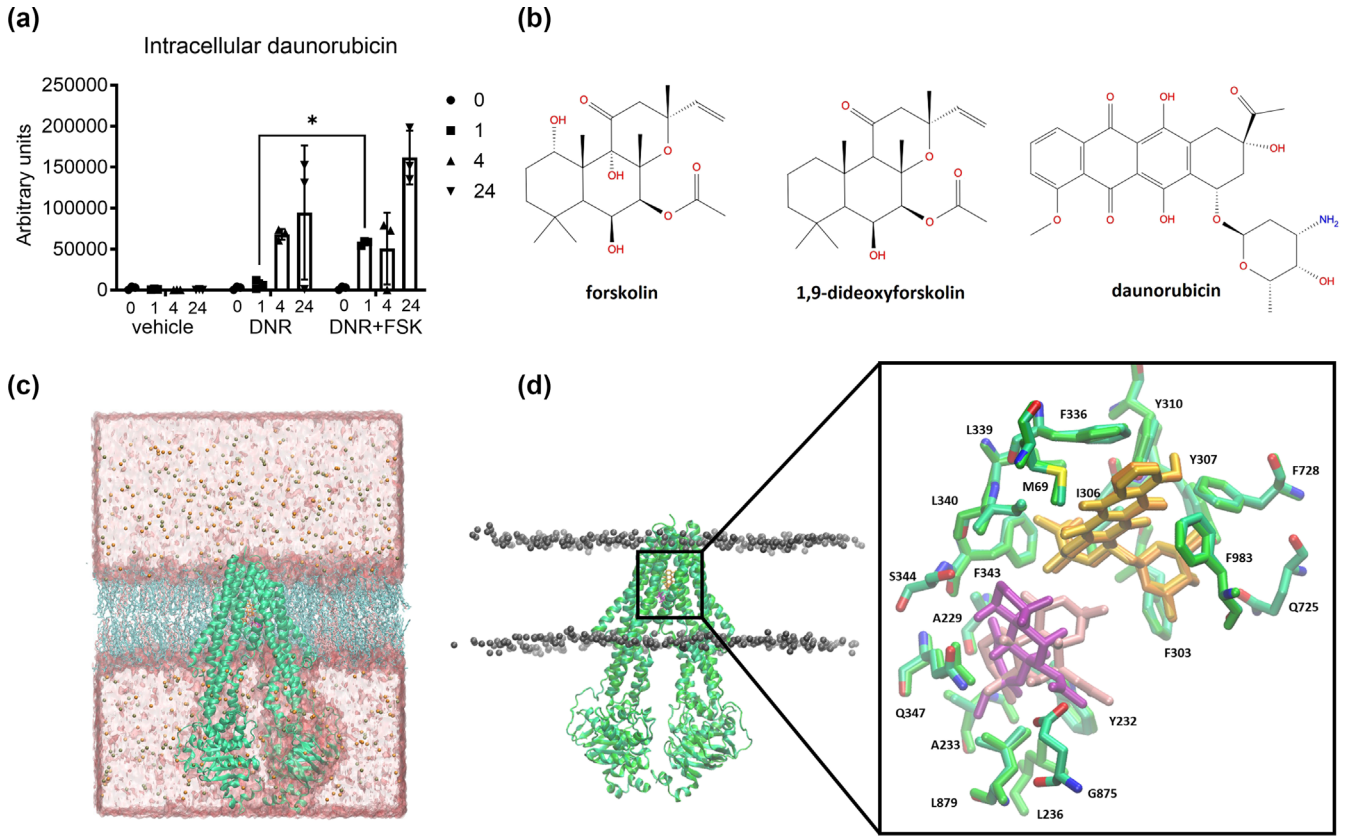

FIGURE 8 Effect of forskolin on P-glycoprotein -mediated daunorubicin export. (a) Analysis of intracellular daunorubicin. MV411 were treated with 40 μM forskolin, 10 nM daunorubicin or combination for 1, 4 and 24 h. The amount of intracellular daunorubicin was measured by LC–MS. Data show mean ± SD of three independent experiments. (b) Molecular structures of the three compounds/drugs docked to P-glycoprotein forskolin, 1,9-dideoxyforskolin and daunorubicin. (c) Cross-sectional illustration of the P-glycoprotein/drug complexes. Cartoon ribbons (in green) embedded in the physiological membrane used in this study. The water box and ionisable salts (grey and orange spheres) are also included in this representation. Here, the binding pocket is occupied with forskolin and daunorubicin. Figures were produced with Maestro 2D sketcher (Schrödinger release 2024-1: Maestro, Schrödinger, LLC, New York, NY) and VMD. (d) Illustration of the comparative binding site of P-glycoprotein. (left) Ribbon depiction of the P-gp binding site with forskolin (purple) and daunorubicin (yellow), superimposed on the P-gp binding site with 1,9-dideoxyforskolin (pink) and daunorubicin (orange). *(right)* a detailed view of the P-gp binding site with forskolin (purple) and daunorubicin (yellow), with crucial residues displayed in light green and labelled accordingly. Corresponding residues in the P-gp binding site with 1,9-dideoxyforskolin (pink) and daunorubicin (orange) are indicated in dark green. Figures were produced with VMD.

5 | DISCUSSION

AML is a heterogenous disease with varying oncogenic drivers that determine distinct outcomes. Given the widespread inactivation of PP2A in AML, its role in regulating signalling pathways fundamental for leukaemogenesis (Goswami et al., 2022), stem cell self-renewal and drug resistance (M. Esposito, 2019; M. T. Esposito et al., 2015; Yeung et al., 2010) and the recent discovery of SET-PP2A pathway as a therapeutic target for *KMT2A*-r leukaemia (Di Mambro et al., 2023), we investigated the expression of PP2A and reasoned that pharmacological strategies aimed at activating PP2A may suppress the leukaemogenesis at multiple nodes. To this aim, we used **forskolin**, a diterpene produced by the roots of the Indian plant *Coleus forskohlii* (Sapio et al., 2017), reported as PP2A activator (Cristobal et al., 2011; Cristóbal et al., 2014; Neviani et al., 2005). The analysis of PP2A-Cα and PP2A-Cβ at transcriptional and protein level indicated that PP2A-Cα is abundantly expressed in primary *KMT2A*-r samples and leukaemic cell lines. *PPP2CA* is located on chromosome 5, whereas *PPP2CB* is located on chromosome 8. Therefore, it is likely that the higher expression of *PPP2CA in KMT2A-r* primary samples than in those with monosomy of chromosome 5 and complex karyotype is because of the loss of one *PPP2CA* allele in these two subtypes. Likewise, the higher mRNA expression of *PPP2CB* in patients with trisomy/tetrasomy 8 and complex karyotype might be because of gene duplication.

Forskolin had a cytostatic and cytotoxic effect on AML leukaemic cells and led to a statistically significant decrease in phospho-ERK1/2 (Tyr202/Thr204), indicating an overall inhibition of ERK1/2 activity, in agreement with another study (Illiano, Sapio, et al., 2018). Forskolin decreased c-MYC protein levels, an effect reported with other PP2A activators, such as OSU-2S (Goswami et al., 2022) and **FTY720** (Di Mambro et al., 2023). Notably, forskolin also induced

transcriptional repression of c-*MYC* and, in the *KMT2A*-r cell line MV411, it decreased the expression of KMT2A target genes *HOXA9* and *HOXA10*. By using RNA interference, our data provide evidence that some of the effects of forskolin on *KMT2A*-r leukaemic cells are dependent on PP2A. Indeed, upon *PPP2CA* knockdown combined with forskolin, the repressive effect of forskolin on c-*MYC* was lost, suggesting that PP2A expression regulates forskolin-mediated transcriptional repression of *c-MYC* and *HOXA10* in *KMT2A*-r leukaemic cells. These effects on *c-MYC* could be the result of the PP2A-mediated inhibition of **ERK1/2** (Letourneux et al., 2006) (Figure 9) that stimulate *c-MYC* transcription via phosphorylation-dependent recruitment of the ETS transcription factors ELK1, ELK3 and ELK4 and via phosphorylation-independent recruitment of cyclin-dependent kinase CDK9 on the promoter of *c-MYC* (Agudo-Ibanez et al., 2023; Vervoort et al., 2021). In addition, this effect could be because of the PP2A-mediated inhibition of **WNT** signalling that regulates *c-MYC* transcription through **β-catenin** (Wagstaff et al., 2022) (Figure 9). As a negative regulator of WNT signalling, PP2A dephosphorylates Axin and APC that are part of **β catenin destruction complex** (Hsu et al., 1999). In this complex Axin and APC bring β-catenin in close proximity to **GSK3β** that phosphorylates β-catenin on Ser33, Ser37 and Thr41, tagging β-catenin for proteasomal degradation. PP2A also regulates GSK3β phosphorylation on Ser9, but it is important to highlight that β-catenin phosphorylation by GS3Kβ is impervious to the GSK3β Ser9 phosphorylation mechanism (Ng et al., 2009). It is interesting to highlight that forskolin was previously reported to regulate the expression of *c-MYC* in non-Hodgkin's lymphomas and to increase the stability of Axin (H. Wang et al., 2019). Whether these effects are dependent on PP2A-mediated dephosphorylation of Axin was not determined; therefore, this warrants further investigation.

Overall, our data point to a PP2A-dependent mechanism of regulation of *c-MYC* in *KMT2A*-r cells which is distinct from the current knowledge indicating PP2A mainly as a regulator of MYC protein stability (Goswami et al., 2022; Pippa & Odero, 2020).

The transcriptional repression of *HOXA9* and *HOXA10* by forskolin is a novel and very interesting finding. A previous study showed that phosphorylation mutants of the transcription factor CREB1 at Ser 133 and Ser 129 and GSK3β inhibitors disrupt the interaction between

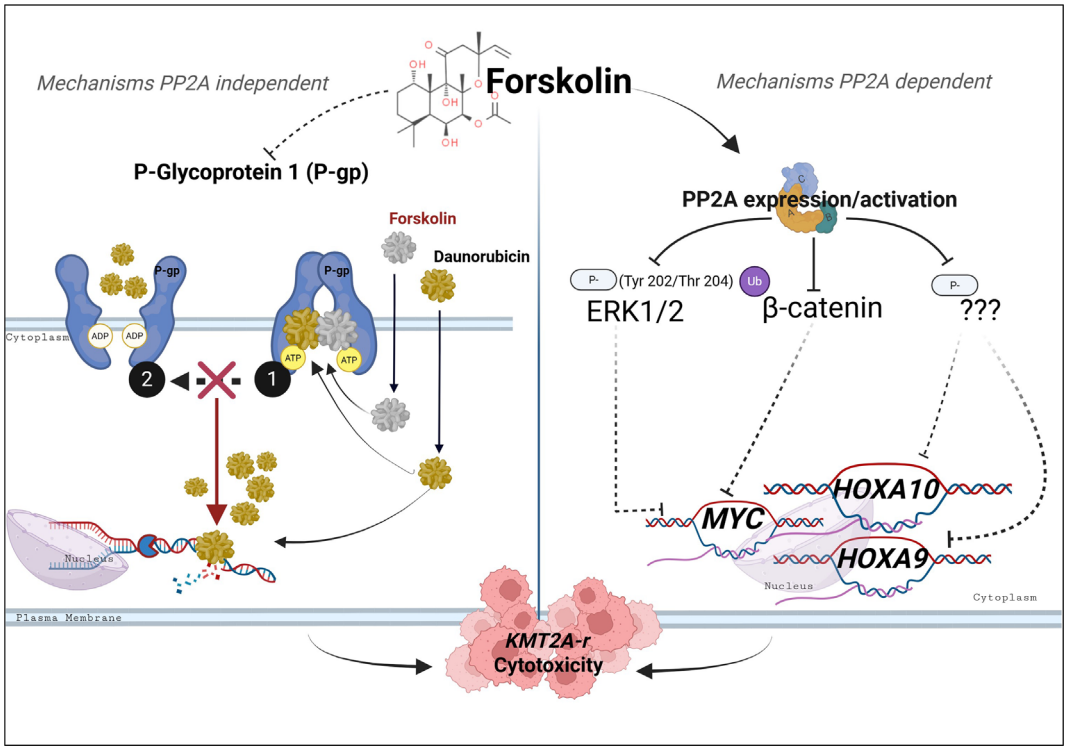

FIGURE 9 Molecular mechanisms underlying forskolin effects in KMT2A-r leukaemic cells. The schematic cartoon represents PP2A-dependent and PP2A-independent effects of forskolin in *KMT2A*-r leukaemia. (right) PP2A-dependent mechanisms: Forskolin rescues the activity of PP2A that targets the phosphorylation of phospho-ERK1/2 (Tyr202/Thr204) and the ubiquitination of β-catenin. The dephosphorylation on ERK1/2 marks the kinase as inactive and leads to transcriptional repression of *c-MYC* in KMT2A-r AML cells. The expression *c-MYC* is also under the control of β-catenin, whose ubiquitination is regulated by the β-catenin destruction complex, modulated by PP2A. Unidentified PP2A-dependent targets regulate the expression of *HOXA9* and *HOXA10*. (left): PP2A-independent mechanisms: forskolin binds the poly-specific drug-binding pocket of the P-glycoprotein (P-gp), a transmembrane ATP-dependent efflux pump. In combination treatment with standard-care daunorubicin, forskolin inhibits the switch from the inward (1) to the outward-facing conformation (2) of P-gp, interfering with active export of daunorubicin n out of the *KMT2A*-r AML cells. This leads to accumulation of daunorubicin inside the *KMT2A*-r AML cells where it intercalates between the DNA strands and prevents the progression of topoisomerase II, thereby halting DNA replication and inducing replication stress and DSBs.

CREB1 and its coactivators **CBP** and TORC with MEIS1, suppressing *HOX*-mediated transcription (Z. Wang et al., 2010), a mechanism consistent with the distinct efficacy of GSK3β inhibitors in *KMT2A*-r leukaemia (Z. Wang et al., 2008; Yeung et al., 2010). However, GSK3β inhibition did not directly impact the expression of *HOXA9* and *HOXA10* (Z. Wang et al., 2010), as, instead, we observed with forskolin; therefore, the precise molecular mechanisms and pathways involved in forskolin-mediated transcriptional control of *HOXA9* and *HOXA10* and the role of PP2A in this context warrant further investigation (Figure 9).

As forskolin is a stimulator of **adenylate cyclase**, we tested whether an analogue of forskolin, 1,9-dideoxy-forskolin, lacking adenylate cyclase activating function, had similar cellular outcomes. Our data indicated that both compounds repress the transcriptional expression of c-*MYC* and *HOXA10* and have similar cytotoxic effects, suggesting that these effects are not dependent on stimulation of adenylate cyclase activation. This is in agreement with a study, published during the revision of this paper, that reported a cAMP-independent repressive effect of forskolin diporate, a water-soluble analogue of forskolin, on *c-MYC* expression in ovarian cancer cells (Knarr et al., 2024). This study and our data highlight that some of the anti-cancer effects of forskolin in ovarian cancer cells and in leukaemic cells are non-canonical and independent of adenylate cyclase activation. In addition, our data provide evidence that forskolin, despite decreasing *PPP2CA* expression, increases the activity of PP2A, although the underlying molecular mechanisms are still not completely elucidated. Two independent groups showed that forskolin is able to activate PP2A by decreasing the inhibitory phosphorylation of PP2A on Tyr307 (Cristobal et al., 2011; Cristóbal et al., 2014; Neviani et al., 2005), a post-translational modification mediated by the **Src family of protein tyrosine kinases** (Chen et al., 1994) and **JAK2** (Yokoyama et al., 2003). However, the antibodies used to detect phospho-PP2A (Tyr307) have been recently objects of scrutiny (Frohner, Mudrak, Schuchner, et al., 2020; Ogris et al., 2018). A more recent study has identified by MS other putative PP2A-C phosphorylations on Tyr127 and Tyr284 in response to Src and **Fyn**, respectively (Sontag et al., 2022). Phosphorylation on Tyr284 alters the specificity of PP2A holoenzyme by promoting the dissociation of the PP2A regulatory Bα subunit (B55α, encoded by *PPP2R2A*) with an overall activating effect on PP2A downstream targets Tau and Erk1/2 (Sontag et al., 2022). It is yet to be determined whether forskolin affects this phospho-site, and whether this mechanism could explain some of its PP2A-dependent anti-cancer effects. Forskolin has also been shown to decrease the phosphorylation of 19 e/α-endosulfine (ENSA) at Ser67, opposing the effect of Greatwall kinase (MASL) and the conversion of ENSA into a PP2A endogenous inhibitor (Kumm et al., 2020). In addition, forskolin can also stimulate PP2A through two cAMP-dependent mechanisms, reviewed in Leslie and Nairn (2019). One pathway is through the PKA and PKG-mediated phosphorylation of the PP2A B56 subunit (Ahn et al., 2007; Feschenko et al., 2002; Yu & Ahn, 2010); the second pathway is through disinhibition of PP2A by PKA-mediated phosphorylation of ARPP-16 (Musante et al., 2017).

We would like to acknowledge that, to measure PP2A activity in cellular extracts, we employed a commercially available immunoprecipitation-based kit used in several studies. A study by Frohner et al. reported that the antibody provided in this kit, against PP2A-C, does not bind non-methylated forms of PP2A-C and suggested that immunoprecipitation with an antibody against PPP2R2A would be a better option to consider the methylation of PP2A-C. We performed our enzymatic activity assays with both antibodies, and the results confirm a stimulatory effect of forskolin on PP2A. Given that both PP2A-C and PP2R2A were repressed by forskolin, the data must be interpreted taking in consideration the limitation of this tool (Frohner, Mudrak, Kronlachner, et al., 2020).

In a few studies, the anti-proliferative effect of forskolin has been shown to be dependent on cAMP (Illiano, Conte, et al., 2018; Illiano, Sapio, et al., 2018). It is not clear whether the anti-proliferative effect reported in these studies depends on PP2A activation.

Consistent with its anti-proliferative effect, forskolin treatment is synergistic with cytotoxic chemotherapeutic agents (Cristobal et al., 2011; Cristóbal et al., 2014; Follin-Arbelet et al., 2015; Illiano, Conte, et al., 2018; Illiano, Sapio, et al., 2018). We therefore tested forskolin in combination with **daunorubicin**, used in induction and consolidation treatment for AML patients. Our results show that forskolin sensitises *KMT2A*-r cells to daunorubicin. Moreover, a cytotoxic effect was also observed, although attenuated, in the presence of BMSCs, which confer drug-resistance mechanisms (Arroyo-Berdugo et al., 2023). Other groups have reported contradictory results. Naderi et al. demonstrated that forskolin inhibits the action of ionising radiation, anthracyclines, alkylating agents and platinum compounds through cAMP (E. Naderi et al., 2009; S. Naderi et al., 2005). Likewise, cAMP elevation has been shown to confer drug resistance via PKA-dependent phosphorylation of Bad and CREB1 (Gausdal et al., 2013; Xiao & Kan, 2017). Our data indicate that forskolin increases the sensitivity of *KMT2A*-r leukaemic cells to daunorubicin, but, in contrast to the data reported by Illiano, Sapio, et al. (2018) in triple negative breast cancer cells, this effect is not dependent on cAMP and PKA activation, because, in our experiments, 1,9-dideoxy-forskolin, similar to forskolin, was able to sensitise the *KMT2A*-r cells to daunorubicin and because pre-incubation with a PKA inhibitor did not decrease the cytotoxic effect of the combination forskolin–daunorubicin. Furthermore, this effect is not dependent on PP2A-Cα as the knockdown of *PPP2CA* did not decrease the cytotoxic effect of the combination forskolin–daunorubicin. As daunorubicin efflux is mediated by active pumps such as **P-glycoprotein**, and forskolin has been shown to interact with P-glycoprotein (Morris et al., 1991; Morris et al., 1994; Safa, 2004), we hypothesised that forskolin might inhibit P-glycoprotein, retaining daunorubicin and other xenobiotics in the cells (Figure 9). Utilising advanced docking protocols and MD simulations, we successfully positioned forskolin, 1,9-dideoxyforskolin and daunorubicin within the P-gp binding site, showing not only that forskolin and 1,9-dideoxyforskolin share the same binding site but also presenting a model where these molecules co-occupy the binding site with daunorubicin, suggesting a shared interaction landscape. This also aligns with the observed experimental EM structure of the P-gp bound to **zosuquidar**, (PDB ID: 7A6F), where there are two molecules of zosuquidar in the binding site (Nosol et al., 2020).

Additionally, by providing a comparing analysis to **vincristine**, a known P-gp substrate with established anti-cancer properties, our results highlight the binding site's adaptability and suggest a potential for synergistic or additive effects when targeting this site with multiple compounds.

6 | CONCLUSIONS

Forskolin, a natural compound with antitumour activity and with minimal toxicity to normal tissues, has a PP2A-dependent cytostatic and cytotoxic effect on *KMT2A*-r cells and represents a valuable therapeutic strategy to target c-MYC, HOXA9 and HOXA10 and increase response to chemotherapy. Our data indicate that the effects of forskolin on *KMT2A*-r cells, including transcriptional repression of *c-MYC* and *HOXA10* and sensitisation to daunorubicin, are not dependent on stimulation of adenylate cyclase. This suggests that it might be possible to uncouple the anti-cancer effects of forskolin from its canonical effects, allowing its use in combination with daunorubicin, to increase the therapeutic index and tolerability of daunorubicin, decreasing morbidity for patients while achieving equivalent clinical response. Further studies are required to address how forskolin activates PP2A and exerts its anti-leukaemogenic effects.

AUTHOR CONTRIBUTIONS

Maria Teresa Esposito and Yoana Arroyo-Berdugo conceived the experimental design. Yoana Arroyo-Berdugo, Antonella Di Mambro, Immacolata Zollo, Volker Behrends and Maria Teresa Esposito performed the experiments and analysed the data. Luca Cozzuto performed RNAseq data analysis and visualisation with input from Julia Ponomarenko. Michelle A Sahai conducted the molecular docking on P-gp. Yolanda Calle provided the experimental models used in this study. Owen Williams, Bela Patel and John Gribben gathered patients' material, PDX and provided clinical data. Bela Patel and Yolanda Calle contributed critical intellectual input in design and interpretation of data. Maria Teresa Esposito conceptualised, supervised the study, provided the funding and wrote and edited the manuscript. All the authors critically reviewed and edited the manuscript.

ACKNOWLEDGEMENTS

We would like to thank Leukaemia UK, the University of Roehampton, the University of Surrey and the Institute of Biomedical Science for funding this study, the patients for donating their samples for research purposes, the tissue bank of Barts Cancer Institute, and Prof. Fulvio D'Acquisto and Prof. Jolanta Opacka-Juffry for their mentoring. The graphical abstract was created in BioRender.com.

CONFLICT OF INTEREST STATEMENT

The authors have no competing financial interests to declare.

DATA AVAILABILITY STATEMENT

The heatmap shown in Figure 1 has been generated by analysing data available from Leucegene (GSE62190, GSE66917, GSE67039).

DECLARATION OF TRANSPARENCY AND SCIENTIFIC RIGOUR

This Declaration acknowledges that this paper adheres to the principles for transparent reporting and scientific rigour of preclinical research as stated in the *BJP* guidelines for Natural Products Research, Design and Analysis, and Immunoblotting and Immunochemistry, and as recommended by funding agencies, publishers and other organisations engaged with supporting research.

ORCID

Maria Teresa Esposito https://orcid.org/0000-0002-9147-6906

REFERENCES

Aasebo, E., Berven, F. S., Bartaula-Brevik, S., Stokowy, T., Hovland, R., Vaudel, M., Døskeland, S. O., McCormack, E., Batth, T. S., Olsen, J. V., Bruserud, Ø., Selheim, F., & Hernandez-Valladares, M. (2020). Proteome and phosphoproteome changes associated with prognosis in acute myeloid leukemia. *Cancers*, *12*(3), 709. https://doi.org/10.3390/cancers12030709

Agudo-Ibanez, L., Morante, M., Garcia-Gutierrez, L., Quintanilla, A., Rodriguez, J., Munoz, A., León, J., & Crespo, P. (2023). ERK2 stimulates MYC transcription by anchoring CDK9 to the MYC promoter in a kinase activity-independent manner. *Science Signaling*, *16*(794), eadg4193. https://doi.org/10.1126/scisignal.adg4193

Ahn, J. H., McAvoy, T., Rakhilin, S. V., Nishi, A., Greengard, P., & Nairn, A. C. (2007). Protein kinase A activates protein phosphatase 2A by phosphorylation of the B56delta subunit. *Proceedings of the National Academy of Sciences of the United States of America*, *104*(8), 2979–2984. https://doi.org/10.1073/pnas.0611532104

Alexander, S. P. H., Fabbro, D., Kelly, E., Mathie, A. A., Peters, J. A., Veale, E. L., Armstrong, J. F., Faccenda, E., Harding, S. D., Davies, J. A., Annett, S., Boison, D., Burns, K. E., Dessauer, C., Gertsch, J., Helsby, N. A., Izzo, A. A., Ostrom, R., Papapetropoulos, A., … Wong, S. S. (2023a). The concise guide to PHARMACOLOGY 2023/24: Enzymes. *British Journal of Pharmacology*, *180*, S289–S373. https://doi.org/10.1111/bph.16181

Alexander, S. P. H., Fabbro, D., Kelly, E., Mathie, A. A., Peters, J. A., Veale, E. L., Armstrong, J. F., Faccenda, E., Harding, S. D., Davies, J. A., Amarosi, L., Anderson, C. M. H., Beart, P. M., Broer, S., Dawson, P. A., Gyimesi, G., Hagenbuch, B., Hammond, J. R., Hancox, J. C., … Verri, T. (2023b). The Concise Guide to PHARMACOLOGY 2023/24: Transporters. *British Journal of Pharmacology*, *180*, S374–S469. https://doi.org/10.1111/bph.16182

Alexander, S. P. H., Roberts, R. E., Broughton, B. R. S., Sobey, C. G., George, C. H., Stanford, S. C., Cirino, G., Docherty, J. R., Giembycz, M. A., Hoyer, D., Insel, P. A., Izzo, A. A., Ji, Y., MacEwan, D. J., Mangum, J., Wonnacott, S., & Ahluwalia, A. (2018). Goals and practicalities of immunoblotting and immunohistochemistry: A guide for submission to the *British Journal of Pharmacology*. *British Journal of Pharmacology*, *175*, 407–411. https://doi.org/10.1111/bph.14112

Arroyo-Berdugo, Y., Sendino, M., Greaves, D., Nojszewska, N., Idilli, O., So, C. W., Di Silvio, L., Quartey-Papafio, R., Farzaneh, F., Rodriguez, J. A., & Calle, Y. (2023). High throughput fluorescence-based in vitro experimental platform for the identification of effective therapies to overcome tumour microenvironment-mediated drug resistance in AML. *Cancers (Basel)*, *15*(7), 1988. https://doi.org/10.3390/cancers15071988

Behrends, V., Tredwell, G. D., & Bundy, J. G. (2011). A software complement to AMDIS for processing GC-MS metabolomic data. *Analytical Biochemistry*, *415*(2), 206–208. https://doi.org/10.1016/j.ab.2011.04.009

Casado, P., Rio-Machin, A., Miettinen, J. J., Bewicke-Copley, F., Rouault-Pierre, K., Krizsan, S., Parsons, A., Rajeeve, V., Miraki-Moud, F., Taussig, D. C., Bödör, C., Gribben, J., Heckman, C., Fitzgibbon, J., & Cutillas, P. R. (2023). Integrative phosphoproteomics defines two biologically distinct groups of KMT2A rearranged acute myeloid leukaemia with different drug response phenotypes. *Signal Transduction and Targeted Therapy*, *8*(1), 80. https://doi.org/10.1038/s41392-022-01288-1

Chen, J., Parsons, S., & Brautigan, D. L. (1994). Tyrosine phosphorylation of protein phosphatase 2A in response to growth stimulation and v-src transformation of fibroblasts. *The Journal of Biological Chemistry*, *269*(11), 7957–7962. https://doi.org/10.1016/S0021-9258(17)37144-2

Choi, C. H. (2005). ABC transporters as multidrug resistance mechanisms and the development of chemosensitizers for their reversal. *Cancer Cell International*, *5*, 30. https://doi.org/10.1186/1475-2867-5-30

Cristobal, I., Garcia-Orti, L., Cirauqui, C., Alonso, M. M., Calasanz, M. J., & Odero, M. D. (2011). PP2A impaired activity is a common event in acute myeloid leukemia and its activation by forskolin has a potent anti-leukemic effect. *Leukemia*, *25*(4), 606–614. https://doi.org/10.1038/leu.2010.294

Cristóbal, I., Rincón, R., Manso, R., Madoz-Gúrpide, J., Caramés, C., del Puerto-Nevado, L., Rojo, F., & García-Foncillas, J. (2014). Hyperphosphorylation of PP2A in colorectal cancer and the potential therapeutic value showed by its forskolin-induced dephosphorylation and activation. *Biochimica et Biophysica Acta (BBA) - Molecular Basis of Disease*, *1842*(9), 1823–1829. https://doi.org/10.1016/j.bbadis.2014.06.032

Curtis, M. J., Alexander, S. P. H., Cortese-Krott, M., Kendall, D. A., Martemyanov, K. A., Mauro, C., Panettieri, R. A. Jr., Papapetropoulos, A., Patel, H. H., Santo, E. E., Schulz, R., Stefanska, B., Stephens, G. J., Teixeira, M. M., Vergnolle, N., Wang, X., & Ferdinandy, P. (2025). Guidance on the planning and reporting of experimental design and analysis. *British Journal of Pharmacology*, *182*(7), 1413–1415. https://doi.org/10.1111/bph.17441

Di Mambro, A., Arroyo-Berdugo, Y., Fioretti, T., Randles, M., Cozzuto, L., Rajeeve, V., Cevenini, A., Austin, M. J., Esposito, G., Ponomarenko, J., Lucas, C. M., Cutillas, P., Gribben, J., Williams, O., Calle, Y., Patel, B., & Esposito, M. T. (2023). SET-pp2a complex as a new therapeutic target in *KMT2A* (MLL) rearranged AML. *Oncogene*, *42*(50), 3670–3683. https://doi.org/10.1038/s41388-023-02840-1

Di Mambro, A., & Esposito, M. T. (2022). Thirty years of SET/-TAF1beta/I2PP2A: From the identification of the biological functions to its implications in cancer and Alzheimer's disease. *Bioscience Reports*, *42*(11), BSR20221280. https://doi.org/10.1042/BSR20221280

Dohner, H., Wei, A. H., & Lowenberg, B. (2021). Towards precision medicine for AML. *Nature Reviews Clinical Oncology*, *18*(9), 577–590. https://doi.org/10.1038/s41571-021-00509-w

Esposito, M. (2019). The impact of PI3-kinase/RAS pathway cooperating mutations in the evolution of *KMT2A*-rearranged leukemia. *HemaSphere*, *3*(3), e195. https://doi.org/10.1097/HS9.0000000000000195

Esposito, M. T., Zhao, L., Fung, T. K., Rane, J. K., Wilson, A., Martin, N., Gil, J., Leung, A. Y., Ashworth, A., & So, C. W. (2015). Synthetic lethal targeting of oncogenic transcription factors in acute leukemia by PARP inhibitors. *Nature Medicine*, *21*(12), 1481–1490. https://doi.org/10.1038/nm.3993

Fang, X., Yu, S. X., Lu, Y., Bast, R. C. Jr., Woodgett, J. R., & Mills, G. B. (2000). Phosphorylation and inactivation of glycogen synthase kinase 3 by protein kinase A. *Proceedings of the National Academy of Sciences of the United States of America*, *97*(22), 11960–11965. https://doi.org/10.1073/pnas.220413597

Feschenko, M. S., Stevenson, E., Nairn, A. C., & Sweadner, K. J. (2002). A novel cAMP-stimulated pathway in protein phosphatase 2A activation. *Journal of Pharmacology and Experimental Therapeutics*, *302*(1), 111–118. https://doi.org/10.1124/jpet.302.1.111

Flare. (2024). V7.2, Cresset, Litlington, Cambridgeshire, UK,. (accessed)

Follin-Arbelet, V., Misund, K., Naderi, E., Ugland, H., Sundan, A., & Blomhoff, H. (2015). The natural compound forskolin synergizes with dexamethasone to induce cell death in myeloma cells via BIM. *Scientific Reports*, *5*(1), 13001. https://doi.org/10.1038/srep13001

Frohner, I. E., Mudrak, I., Kronlachner, S., Schüchner, S., & Ogris, E. (2020). Antibodies recognizing the C terminus of PP2A catalytic subunit are unsuitable for evaluating PP2A activity and holoenzyme composition. *Science Signaling*, *13*(616), eaax6490. https://doi.org/10.1126/scisignal.aax6490

Frohner, I. E., Mudrak, I., Schuchner, S., Anrather, D., Hartl, M., Sontag, J. M., Wadzinski, B. E., Preglej, T., Ellmeier, W., & Ogris, E. (2020). PP2A(C) phospho-Tyr(307) antibodies are not specific for this modification but are sensitive to other PP2A(C) modifications including Leu(309) methylation. *Cell Reports*, *30*(9), 3171–3182. https://doi.org/10.1016/j.celrep.2020.02.035

Gausdal, G., Wergeland, A., Skavland, J., Nguyen, E., Pendino, F., Rouhee, N., McCormack, E., Herfindal, L., Kleppe, R., Havemann, U., Schwede, F., & Doskeland, S. O. (2013). Cyclic AMP can promote APL progression and protect myeloid leukemia cells against anthracycline-induced apoptosis. *Cell Death & Disease*, *4*(2), e516. https://doi.org/10.1038/cddis.2013.39

Gosline, S. J. C., Tognon, C., Nestor, M., Joshi, S., Modak, R., Damnernsawad, A., Posso, C., Moon, J., Hansen, J. R., Hutchinson-Bunch, C., Pino, J. C., Gritsenko, M. A., Weitz, K. K., Traer, E., Tyner, J., Druker, B., Agarwal, A., Piehowski, P., McDermott, J. E., & Rodland, K. (2022). Proteomic and phosphoproteomic measurements enhance ability to predict ex vivo drug response in AML. *Clinical Proteomics*, *19*(1), 30. https://doi.org/10.1186/s12014-022-09367-9

Goswami, S., Mani, R., Nunes, J., Chiang, C. L., Zapolnik, K., Hu, E., Frissora, F., Mo, X., Walker, L. A., Yan, P., Bundschuh, R., Beaver, L., Devine, R., Tsai, Y. T., Ventura, A., Xie, Z., Chen, M., Lapalombella, R., Walker, A., … Muthusamy, N. (2022). PP2A is a therapeutically targetable driver of cell fate decisions via a c-Myc/p21 axis in human and murine acute myeloid leukemia. *Blood*, *139*(9), 1340–1358. https://doi.org/10.1182/blood.2020010344

Hsu, W., Zeng, L., & Costantini, F. (1999). Identification of a domain of Axin that binds to the serine/threonine protein phosphatase 2A and a self-binding domain. *Journal of Biological Chemistry*, *274*(6), 3439–3445. https://doi.org/10.1074/jbc.274.6.3439

Illiano, M., Conte, M., Sapio, L., Nebbioso, A., Spina, A., Altucci, L., & Naviglio, S. (2018). Forskolin sensitizes human acute myeloid leukemia cells to H3K27me2/3 demethylases GSKJ4 inhibitor via protein kinase A. *Frontiers in Pharmacology*, *9*, 792. https://doi.org/10.3389/fphar.2018.00792

Illiano, M., Sapio, L., Salzillo, A., Capasso, L., Caiafa, I., Chiosi, E., Spina, A., & Naviglio, S. (2018). Forskolin improves sensitivity to doxorubicin of triple negative breast cancer cells via protein kinase A-mediated ERK1/2 inhibition. *Biochemical Pharmacology*, *152*, 104–113. https://doi.org/10.1016/j.bcp.2018.03.023

Izzo, A. A., Teixeira, M., Alexander, S. P. H., Cirino, G., Docherty, J. R., George, C. H., Insel, P. A., Ji, Y., Kendall, D. A., Panettieri, R. A., Sobey, C. G., Stanford, S. C., Stefanska, B., Stephens, G., & Ahluwalia, A. (2020). A practical guide for transparent reporting of research on natural products in the British Journal of pharmacology: Reproducibility of natural product research. *British Journal of Pharmacology*, *177*(10), 2169–2178. https://doi.org/10.1111/bph.15054

Jo, S., Kim, T., Iyer, V. G., & Im, W. (2008). CHARMM-GUI: A web-based graphical user interface for CHARMM. *Journal of Computational Chemistry*, *29*(11), 1859–1865. https://doi.org/10.1002/jcc.20945

Jo, S., Lim, J. B., Klauda, J. B., & Im, W. (2009). CHARMM-GUI membrane builder for mixed bilayers and its application to yeast membranes.

Biophysical Journal, *97*(1), 50–58. https://doi.org/10.1016/j.bpj.2009.04.013

Kandoth, C., McLellan, M. D., Vandin, F., Ye, K., Niu, B., Lu, C., Xie, M., Zhang, Q., McMichael, J. F., Wyczalkowski, M. A., Leiserson, M. D. M., Miller, C. A., Welch, J. S., Walter, M. J., Wendl, M. C., Ley, T. J., Wilson, R. K., Raphael, B. J., & Ding, L. (2013). Mutational landscape and significance across 12 major cancer types. *Nature*, *502*(7471), 333–339. https://doi.org/10.1038/nature12634

Kanne, H., Burte, N. P., Prasanna, V., & Gujjula, R. (2015). Extraction and elemental analysis of *Coleus forskohlii* extract. *Pharmacognosy Research*, *7*(3), 237–241. https://doi.org/10.4103/0974-8490.157966

Kauko, O., & Westermarck, J. (2018). Non-genomic mechanisms of protein phosphatase 2A (PP2A) regulation in cancer. *The International Journal of Biochemistry & Cell Biology*, *96*, 157–164. https://doi.org/10.1016/j.biocel.2018.01.005

Kim, R. B. (2002). Drugs as P-glycoprotein substrates, inhibitors, and inducers. *Drug Metabolism Reviews*, *34*(1–2), 47–54. https://doi.org/10.1081/dmr-120001389

Knarr, M. J., Moon, J., Rawat, P., DiFeo, A., Hoon, D. S. B., & Drapkin, R. (2024). Repurposing colforsin daropate to treat MYC-driven high-grade serous ovarian carcinomas. *Science Signaling*, *17*(863), eado8303. https://doi.org/10.1126/scisignal.ado8303

Kramer, M. H., Zhang, Q., Sprung, R., Day, R. B., Erdmann-Gilmore, P., Li, Y., Xu, Z., Helton, N. M., George, D. R., Mi, Y., Westervelt, P., Payton, J. E., Ramakrishnan, S. M., Miller, C. A., Link, D. C., DiPersio, J. F., Walter, M. J., Townsend, R. R., & Ley, T. J. (2022). Proteomic and phosphoproteomic landscapes of acute myeloid leukemia. *Blood*, *140*(13), 1533–1548. https://doi.org/10.1182/blood.2022016033

Kumm, E. J., Pagel, O., Gambaryan, S., Walter, U., Zahedi, R. P., Smolenski, A., & Jurk, K. (2020). The cell cycle checkpoint system MAST(L)-ENSA/ARPP19-PP2A is targeted by cAMP/PKA and cGMP/PKG in anucleate human platelets. *Cells*, *9*(2), 472. https://doi.org/10.3390/cells9020472

Lavallee, V. P., Baccelli, I., Krosl, J., Wilhelm, B., Barabe, F., Gendron, P., Boucher, G., Lemieux, S., Marinier, A., Meloche, S., Hébert, J., & Sauvageau, G. (2015). The transcriptomic landscape and directed chemical interrogation of MLL-rearranged acute myeloid leukemias. *Nature Genetics*, *47*(9), 1030–1037. https://doi.org/10.1038/ng.3371

Leslie, S. N., & Nairn, A. C. (2019). cAMP regulation of protein phosphatases PP1 and PP2A in brain. *Biochimica et Biophysica Acta (BBA) - Molecular Cell*, *1866*(1), 64–73. https://doi.org/10.1016/j.bbamcr.2018.09.006

Letourneux, C., Rocher, G., & Porteu, F. (2006). B56-containing PP2A dephosphorylate ERK and their activity is controlled by the early gene IEX-1 and ERK. *The EMBO Journal*, *25*(4), 727–738. https://doi.org/10.1038/sj.emboj.7600980

Meyer, C., Larghero, P., Almeida Lopes, B., Burmeister, T., Groger, D., Sutton, R., Venn, N. C., Cazzaniga, G., Corral Abascal, L., Tsaur, G., Fechina, L., Emerenciano, M., Pombo-de-Oliveira, M. S., Lund-Aho, T., Lundán, T., Montonen, M., Juvonen, V., Zuna, J., Trka, J., … Marschalek, R. (2023). The KMT2A recombinome of acute leukemias in 2023. *Leukemia*, *37*(5), 988–1005. https://doi.org/10.1038/s41375-023-01877-1

Miyamoto, R., Kanai, A., Okuda, H., Komata, Y., Takahashi, S., Matsui, H., Inaba, T., & Yokoyama, A. (2021). *HOXA9* promotes *MYC*-mediated leukemogenesis by maintaining gene expression for multiple anti-apoptotic pathways. *eLife*, *10*, e64148. https://doi.org/10.7554/eLife.64148

Morris, D. I., Greenberger, L. M., Bruggemann, E. P., Cardarelli, C., Gottesman, M. M., Pastan, I., & Seamon, K. B. (1994). Localization of the forskolin labeling sites to both halves of P-glycoprotein: Similarity of the sites labeled by forskolin and prazosin. *Molecular Pharmacology*, *46*(2), 329–337. https://doi.org/10.1016/S0026-895X(25)09687-7

Morris, D. I., Speicher, L. A., Ruoho, A. E., Tew, K. D., & Seamon, K. B. (1991). Interaction of forskolin with the P-glycoprotein multidrug transporter. *Biochemistry*, *30*(34), 8371–8379. https://doi.org/10.1021/bi00098a014

Musante, V., Li, L., Kanyo, J., Lam, T. T., Colangelo, C. M., Cheng, S. K., Brody, A. H., Greengard, P., Le Novère, N., & Nairn, A. C. (2017). Reciprocal regulation of ARPP-16 by PKA and MAST3 kinases provides a cAMP-regulated switch in protein phosphatase 2A inhibition. *eLife*, *6*, e24998. https://doi.org/10.7554/eLife.24998

Naderi, E., Findley, H. W., Ruud, E., Blomhoff, H., & Naderi, S. (2009). Activation of cAMP signaling inhibits DNA damage–induced apoptosis in BCP-ALL cells through abrogation of p53 accumulation. *Blood*, *114*(3), 608–618. https://doi.org/10.1182/blood-2009-02-204883

Naderi, S., Wang, J. Y., Chen, T. T., Gutzkow, K. B., & Blomhoff, H. K. (2005). cAMP-mediated inhibition of DNA replication and S phase progression: Involvement of Rb, p21Cip1, and PCNA. *Molecular Biology of the Cell*, *16*(3), 1527–1542. https://doi.org/10.1091/mbc.e04-06-0501

Neviani, P., Santhanam, R., Trotta, R., Notari, M., Blaser, B. W., Liu, S., Mao, H., Chang, J. S., Galietta, A., Uttam, A., Roy, D. C., Valtieri, M., Bruner-Klisovic, R., Caligiuri, M. A., Bloomfield, C. D., Marcucci, G., & Perrotti, D. (2005). The tumor suppressor PP2A is functionally inactivated in blast crisis CML through the inhibitory activity of the BCR/-ABL-regulated SET protein. *Cancer Cell*, *8*(5), 355–368. https://doi.org/10.1016/j.ccr.2005.10.015

Ng, S. S., Mahmoudi, T., Danenberg, E., Bejaoui, I., de Lau, W., Korswagen, H. C., Schutte, M., & Clevers, H. (2009). Phosphatidylinositol 3-kinase signaling does not activate the Wnt cascade. *Journal of Biological Chemistry*, *284*(51), 35308–35313. https://doi.org/10.1074/jbc.M109.078261

Nosol, K., Romane, K., Irobalieva, R. N., Alam, A., Kowal, J., Fujita, N., & Locher, K. P. (2020). Cryo-EM structures reveal distinct mechanisms of inhibition of the human multidrug transporter ABCB1. *Proceedings of the National Academy of Sciences of the United States of America*, *117*(42), 26245–26253. https://doi.org/10.1073/pnas.2010264117

Ogris, E., Sontag, E., Wadzinski, B., & Narla, G. (2018). Specificity of research antibodies: "Trust is good, validation is better". *Human Pathology*, *72*, 199–201. https://doi.org/10.1016/j.humpath.2017.12.003

Phillips, J. C., Braun, R., Wang, W., Gumbart, J., Tajkhorshid, E., Villa, E., Chipot, C., Skeel, R. D., Kalé, L., & Schulten, K. (2005). Scalable molecular dynamics with NAMD. *Journal of Computational Chemistry*, *26*(16), 1781–1802. https://doi.org/10.1002/jcc.20289

Pippa, R., & Odero, M. D. (2020). The role of MYC and PP2A in the initiation and progression of myeloid leukemias. *Cells*, *9*(3), 544. https://doi.org/10.3390/cells9030544

Ramaswamy, K., Spitzer, B., & Kentsis, A. (2015). Therapeutic re-activation of protein phosphatase 2A in acute myeloid leukemia. *Frontiers in Oncology*, *5*, 16. https://doi.org/10.3389/fonc.2015.00016

Safa, A. R. (2004). Identification and characterization of the binding sites of P-glycoprotein for multidrug resistance-related drugs and modulators. *Current Medicinal Chemistry. Anti-Cancer Agents*, *4*(1), 1–17. https://doi.org/10.2174/1568011043482142

Sapio, L., Gallo, M., Illiano, M., Chiosi, E., Naviglio, D., Spina, A., & Naviglio, S. (2017). The natural cAMP elevating compound forskolin in cancer therapy: Is it time? *Journal of Cellular Physiology*, *232*(5), 922–927. https://doi.org/10.1002/jcp.25650

Sontag, J. M., Schuhmacher, D., Taleski, G., Jordan, A., Khan, S., Hoffman, A., Gomez, R. J., Mazalouskas, M. D., Hanks, S. K., Spiller, B. W., Sontag, E., & Wadzinski, B. E. (2022). A new paradigm for regulation of protein phosphatase 2A function via Src and Fyn kinase-mediated tyrosine phosphorylation. *Journal of Biological Chemistry*, *298*(8), 102248. https://doi.org/10.1016/j.jbc.2022.102248

Takahashi, S. (2023). Combination therapies with kinase inhibitors for acute myeloid leukemia treatment. *Hematology Reports*, *15*(2), 331–346. https://doi.org/10.3390/hematolrep15020035

Tazi, Y., Arango-Ossa, J. E., Zhou, Y., Bernard, E., Thomas, I., Gilkes, A., Freeman, S., Pradat, Y., Johnson, S. J., Hills, R., Dillon, R., Levine, M. F., Leongamornlert, D., Butler, A., Ganser, A., Bullinger, L., Döhner, K., Ottmann, O., Adams, R., … Papaemmanuil, E. (2022). Unified classification and risk-stratification in acute myeloid leukemia. *Nature Communications*, *13*(1), 4622. https://doi.org/10.1038/s41467-022-32103-8

Thangapandian, S., Kapoor, K., & Tajkhorshid, E. (2020). Probing cholesterol binding and translocation in P-glycoprotein. *Biochimica et Biophysica Acta*, *1862*(1), 183090. https://doi.org/10.1016/j.bbamem.2019.183090

Vervoort, S. J., Welsh, S. A., Devlin, J. R., Barbieri, E., Knight, D. A., Offley, S., Bjelosevic, S., Costacurta, M., Todorovski, I., Kearney, C. J., Sandow, J. J., & Johnstone, R. W. (2021). The PP2A-integrator-CDK9 axis fine-tunes transcription and can be targeted therapeutically in cancer. *Cell*, *184*(12), 3143–3162. https://doi.org/10.1016/j.cell.2021.04.022

Wagstaff, M., Coke, B., Hodgkiss, G. R., & Morgan, R. G. (2022). Targeting beta-catenin in acute myeloid leukaemia: Past, present, and future perspectives. *Bioscience Reports*, *42*(4), BSR20211841. https://doi.org/10.1042/BSR20211841

Wang, H., Lou, C., & Ma, N. (2019). Forskolin exerts anticancer roles in non-Hodgkin's lymphomas via regulating Axin/beta-catenin signaling pathway. *Cancer Management and Research*, *11*, 1685–1696. https://doi.org/10.2147/CMAR.S180754

Wang, Y. H., Li, Y., Yang, S. L., & Yang, L. (2005). Classification of substrates and inhibitors of P-glycoprotein using unsupervised machine learning approach. *Journal of Chemical Information and Modeling*, *45*(3), 750–757. https://doi.org/10.1021/ci050041k

Wang, Z., Iwasaki, M., Ficara, F., Lin, C., Matheny, C., Wong, S. H., Wong, S. H. K., Smith, K. S., & Cleary, M. L. (2010). GSK-3 promotes conditional association of CREB and its coactivators with MEIS1 to facilitate HOX-mediated transcription and oncogenesis. *Cancer Cell*, *17*(6), 597–608. https://doi.org/10.1016/j.ccr.2010.04.024

Wang, Z., Smith, K. S., Murphy, M., Piloto, O., Somervaille, T. C., & Cleary, M. L. (2008). Glycogen synthase kinase 3 in MLL leukaemia maintenance and targeted therapy. *Nature*, *455*(7217), 1205–1209. https://doi.org/10.1038/nature07284

Winters, A. C., & Bernt, K. M. (2017). MLL-rearranged leukemias-an update on science and clinical approaches. *Frontiers in Pediatrics*, *5*(4). https://doi.org/10.3389/fped.2017.00004

Xiao, L. Y., & Kan, W. M. (2017). Cyclic AMP (cAMP) confers drug resistance against DNA damaging agents via PKAIA in CML cells. *European Journal of Pharmacology*, *794*, 201–208. https://doi.org/10.1016/j.ejphar.2016.11.043

Xing, Y., Xu, Y., Chen, Y., Jeffrey, P. D., Chao, Y., Lin, Z., Li, Z., Strack, S., Stock, J. B., & Shi, Y. (2006). Structure of protein phosphatase 2A core enzyme bound to tumor-inducing toxins. *Cell*, *127*(2), 341–353. https://doi.org/10.1016/j.cell.2006.09.025

Yeh, E., Cunningham, M., Arnold, H., Chasse, D., Monteith, T., Ivaldi, G., Hahn, W. C., Stukenberg, P. T., Shenolikar, S., Uchida, T., Counter, C. M., Nevins, J. R., Means, A. R., & Sears, R. (2004). A signalling pathway controlling c-Myc degradation that impacts oncogenic transformation of human cells. *Nature Cell Biology*, *6*(4), 308–318. https://doi.org/10.1038/ncb1110

Yeung, J., Esposito, M. T., Gandillet, A., Zeisig, B. B., Griessinger, E., Bonnet, D., & So, C. W. (2010). Beta-catenin mediates the establishment and drug resistance of MLL leukemic stem cells. *Cancer Cell*, *18*(6), 606–618. https://doi.org/10.1016/j.ccr.2010.10.032

Yokoyama, N., Reich, N. C., & Miller, W. T. (2003). Determinants for the interaction between Janus kinase 2 and protein phosphatase 2A. *Archives of Biochemistry and Biophysics*, *417*(1), 87–95. https://doi.org/10.1016/s0003-9861(03)00333-3

Yu, U. Y., & Ahn, J. H. (2010). Phosphorylation on the PPP2R5D B regulatory subunit modulates the biochemical properties of protein phosphatase 2A. *BMB Reports*, *43*(4), 263–267. https://doi.org/10.5483/bmbrep.2010.43.4.263

Zeino, M., Saeed, M. E., Kadioglu, O., & Efferth, T. (2014). The ability of molecular docking to unravel the controversy and challenges related to P-glycoprotein—A well-known, yet poorly understood drug transporter. *Investigational New Drugs*, *32*(4), 618–625. https://doi.org/10.1007/s10637-014-0098-1

SUPPORTING INFORMATION

Additional supporting information can be found online in the Supporting Information section at the end of this article.

How to cite this article: Arroyo-Berdugo, Y., Di Mambro, A., Behrends, V., Sahai, M. A., Cozzuto, L., Zollo, I., Ponomarenko, J., Williams, O., Gribben, J., Calle, Y., Patel, B., & Esposito, M. T. (2025). 'Exploiting PP2A dependent and independent effects of forskolin for therapeutic targeting of KMT2A (MLL)-rearranged acute leukaemia'. *British Journal of Pharmacology*, 1–20. https://doi.org/10.1111/bph.70158